TECHNISCHE UNIVERSITÄT WIEN

DIPLOMARBEIT

Interaction in the Model of Topological Fermions

ausgeführt am
Atominstitut
der österreichischen Universitäten

unter der Anleitung von
Ao.Univ.Prof. Dipl.-Ing. Dr.techn. Manfried Faber

durch
Joachim Wabnig
Puchheimstraße 8
3820 Raabs/Thaya

Wien, am

Abstract

The soliton solutions to the 1+1 dimensional sine-Gordon system show the behavior of particles. We consider here a generalization of this model to 3+1 dimensions, the Model of Topological Fermions (MTF) with an inherent length scale r_0. The basic field of this model is an SU(2) field, parametrising an S^3. There is also an additional parameter m, giving the form of the potential, that stabilizes the soliton solution.

We show that the model is equivalent to Maxwell's electrodynamics for the limit of large distances $r \gg r_0$. Then the degrees of freedom are confined to an S^2. We can derive Maxwell's equations from the action of the MTF in this limit, if we introduce a special kind of variation, where we allow only variations along the S^2. Due to topology only quantized charges are allowed in the derived Maxwell equations. By introducing a gauge transformation we can relate the SU(2) connection field to the U(1) gauge potential from electrodynamics. We also show the equivalence of the field strength tensors.

We then turn to the two particle system, especially to a particle anti-particle system. This system is axially symmetric and so we can derive a simplified expression for the energy density. We can also write down the field of the system in the limit $r \gg r_0$. We show how an effect similar to running coupling comes out of the sine-Gordon model. We then look at this effect in the MTF using numerical calculations. By a routine that minimizes the energy in a system where the positions of the soliton cores are fixed we obtain solutions for different parameters in the potential. We also investigate the energy difference between two topologically different states, that are possible in the model.

“The electron is not as simple as it looks”

William Lawrence Bragg (1890-1971)

Contents

1 Introduction **1**
- 1.1 Fermions and Bosons . . . 1
- 1.2 The Model of Topological Fermions (MTF) . . . 2
  - 1.2.1 Differential Geometry on the S^3 . . . 2
  - 1.2.2 Four Dimensional Formulation . . . 4

2 From Soliton Fields to Maxwell's Electromagnetism **6**
- 2.1 Where is the Electromagnetism . . . 6
- 2.2 Solution for one Particle . . . 7
  - 2.2.1 Formulation in SI-Units . . . 8
- 2.3 The Inhomogeneous Maxwell Equations . . . 8
- 2.4 The Homogenous Maxwell Equations Derived from a Variational Principle . . . 10
- 2.5 The Homogenous Maxwell Equations Derived from the Equations of Motion . . . 12
- 2.6 The Coupling of a Point Particle to a Soliton Field in the Electrodynamical Limit . . . 13
- 2.7 Gauging Away the Internal Degrees of Freedom . . . 14
  - 2.7.1 A Special Case: One Particle . . . 15
  - 2.7.2 The General Case . . . 15

3 The Two Particle System **19**
- 3.1 Possible One Particle States . . . 19
- 3.2 Fitting the Fields Together . . . 19
- 3.3 Topologically Different States . . . 21
- 3.4 The Electron-Positron System . . . 21
  - 3.4.1 Energy Densities for the Electron Positron System . . . 21
  - 3.4.2 Electric Field from an Axially Symmetric Soliton Field . . . 26
  - 3.4.3 The $\mathbf{n}$-field at large distances $r \gg r_0$ calculated from the dual potential . . . 26

4 Numerical Calculations **30**
- 4.1 Basic Configuration . . . 30

4.2 Calculation of the Energy 31
4.2.1 Derivatives on a Lattice 31
4.2.2 Summation over the Lattice 32
4.3 Boundary Conditions and Starting Configuration 33
4.4 Calculating the Energy Contribution Outside the Box 34
4.5 Problems due to Numerics 35

5 Running Coupling **36**
5.1 The Sine-Gordon Model 36
5.1.1 Short Introduction to the Model[1] 36
5.1.2 Running Coupling in the Sine-Gordon Model 38

6 Results **41**
6.1 Preparations 41
6.2 Energies for the interacting particles 42

7 Conclusion and outlook **49**

A Field configurations and Pictures **51**

Chapter 1

Introduction

1.1 Fermions and Bosons

In the well established theory of quantum electrodynamics there are two different kinds of particles. The fermions are responsible for the solid matter as we know it and bosons (i.e. the photons in QED) act as messengers between the fermions, creating a force between charged particles. Fermions have some distinct features. They are either neutral or carry a charge, an integer multiple of some number, the elementary charge. They also have half integer spin. There is no theoretical explanation either for the quantization of the charge or how the spin emerges. But there is a relationship between spin and the Pauli exclusion principle.

Let us now take a look at a simple 1+1 dimensional model, that exhibits some of the particle properties mentioned above: The sine-Gordon model (e.g. [1]). Basically it is the mathematical description of a spring-coupled chain of pendula under the influence of gravitation. There exist two different classes of solutions for this model. For small angles of deflection the equation reduces to the Klein-Gordon equation with its usual wave solutions. But one can look at the other extreme. If we take all the pendula right of the middle once around their rotation point we have created a topological excitation, a soliton. This object is stable, even when it moves. It has also some other properties:

- There are two different kinds of solitons, depending on the direction of the winding. We will call them kinks and anti-kinks.
- Kinks and Anti-kinks can annihilate. No soliton remains, only some waves propagating outward from the place of the collision.
- Two kinks cannot be at the same place at one time.

This seems to be the behavior of fermions! There even exists an exact correspondence between the quantized version of the sine-Gordon model and the Thirring model, a quantum field theory in 1+1 dimensions.

Figure 1.1: Collision between two kinks realized in a mechanical model [1]

1.2 The Model of Topological Fermions (MTF)

Now we want to generalize the idea of the sine-Gordon model to our four-dimensional world. This has been done in [2] and we will give a short introduction to this model.

1.2.1 Differential Geometry on the S^3

The underlying field of the MTF parametrises the surface of a four-dimensional sphere, the S^3. We can write it as

$$Q = q_0 + iq_k\sigma_k \tag{1.1}$$

where σ_k are the Pauli matrices. Additionally the condition

$$q_0^2 + \mathbf{q}^2 = 1 \tag{1.2}$$

must hold. An alternative parametrisation is

$$q_0 = \cos\alpha \quad q_k = n_k \sin\alpha \quad \mathbf{n}^2 = 1 \tag{1.3}$$

We can define a scalar product between two fields Q and P in the following way

$$Q \cdot P = q_0 p_0 + \mathbf{q} \cdot \mathbf{p} = \frac{1}{2}\,\mathrm{Tr}(QP^\dagger) \tag{1.4}$$

In the tangential plane we can define a coordinate basis consisting of three orthonormal basis vectors $\sigma_k^Q = \sigma_k Q$ where σ_k are the three Pauli matrices. We can show that the basis vectors lie in the tangential plane by applying the scalar product

$$\sigma_k^Q \cdot Q = \frac{1}{2}\,\mathrm{Tr}(\sigma_k Q Q^\dagger) = 0 \tag{1.5}$$

since the Pauli matrices are traceless. Their orthonormality can also be shown by a scalar product.

$$\sigma_k^Q \cdot \sigma_l^Q = \frac{1}{2}\,\mathrm{Tr}(\sigma_k Q Q^\dagger \sigma_l) = \frac{1}{2}\,\mathrm{Tr}(\sigma_k \sigma_l) = \delta_{kl} \tag{1.6}$$

We can relate the tangent space spanned by the σ_k^Q to the tangent space as it is defined in differential geometry. When we look at how the field Q changes when we move along a curve parametrised by the parameter s we know the derivative lies in the tangent space. We can write it therefore as a linear combination of the basis vectors

$$\partial_s Q = i\Gamma_{sk}\sigma_k^Q \tag{1.7}$$

Now we want to know what this change looks like in a fixed coordinate frame. We choose the basis at the north pole. By multiplying from the right with $Q^\dagger$ we get

$$(\partial_s Q)Q^\dagger = i\Gamma_{sk}\sigma_k Q Q^\dagger = i\Gamma_{sk}\sigma_k \tag{1.8}$$

The coefficients Γ_{sk} tell us how the rotation of the coordinate basis changes Q. We identify Γ_{sk} with the connection coefficients from differential geometry. Using the definition for Q (eq. (1.1)), we can rewrite equation (1.8) and read off the connection coefficients.

$$(\partial_s q_0 + i\sigma_k \partial_s q_k)(q_0 - i\sigma_i q_i) = i\sigma_k(-q_0\partial_s q_k + q_k \partial_s q_0 - \varepsilon_{kij} q_i \partial_s q_j) \tag{1.9}$$

with $q_0\partial_s q_0 + \mathbf{q}\cdot\partial_s\mathbf{q} = 0$ due to orthogonality. We get

$$\mathbf{\Gamma}_s = -q_0\partial_s\mathbf{q} + \mathbf{q}\partial_s q_0 - \mathbf{q}\times\partial_s\mathbf{q} \tag{1.10}$$

We can write the connection in adjoint representation with the generators

$$(T_j)_{kl} = -i\varepsilon_{jkl} \tag{1.11}$$

as

$$\Gamma_s = \mathbf{\Gamma_s}\cdot\mathbf{T}. \tag{1.12}$$

Now we can define a field strength in the usual way written down in matrix form

$$R_{st} = -\partial_s\Gamma_t + \partial_t\Gamma_s + i[\Gamma_s, \Gamma_t] \tag{1.13}$$

or after the removal of the generators

$$\mathbf{R}_{st} = -\partial_s\mathbf{\Gamma_t} + \partial_\mathbf{t}\mathbf{\Gamma_s} - \mathbf{\Gamma_s}\times\mathbf{\Gamma_t} \tag{1.14}$$

With the Maurer-Cartan structure equation in matrix form

$$\partial_s\Gamma_t - \partial_t\Gamma_s = 2i[\Gamma_s, \Gamma_t] \tag{1.15}$$

we get several expressions for the field strength

$$R_{st} = \begin{array}{c} -\partial_s\Gamma_t + \partial_t\Gamma_s + i[\Gamma_s, \Gamma_t] = \frac{1}{2}(-\partial_s\Gamma_t + \partial_t\Gamma_s) = -i[\Gamma_s, \Gamma_t] = \\ = (\mathbf{\Gamma_s} \times \mathbf{\Gamma_t}) \cdot \mathbf{T} \end{array} \tag{1.16}$$

There is a geometric interpretation for the field strength. We see in equation (1.16), that we can express the field strength tensor as the cross product of the connection fields. But the cross product also gives the area spanned by two vectors. So we can read equation (1.16) in the following way: The field strength is the area in internal space spanned by the two connections. Depending on the direction, that we consider in Minkowski space, we get different connections and therefore different areas in internal space. (see Figure).

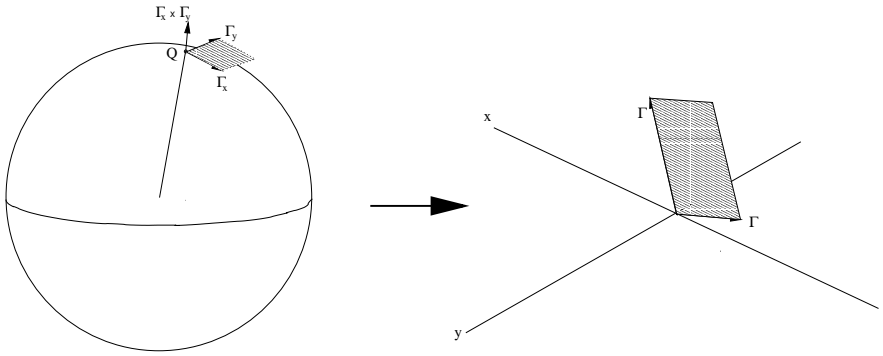

Figure 1.2: The connections for the x- and the y-direction at a certain point on the S^3, denoted by Q. The field strength at this point is the area spanned by the connections, mathematically expressed by the cross product. This area is related by the infinitesimal line elements to the area in Minkowski space.

1.2.2 Four Dimensional Formulation

With the field strength we can write down a Lagrangian density for the model. We change over from the abstract directions s and t to the directions in Minkowski space μ and ν. We also introduce a potential to stabilize our solutions. With the correct constants in front the Lagrangian density now reads

$$\mathcal{L} = -\frac{\alpha_f \hbar c}{4\pi}\left(\frac{1}{8}\mathrm{Tr}(R_{\mu\nu}R^{\mu\nu}) + \frac{1}{r_0^4}q_0^{2m}\right) \tag{1.17}$$

The first part is the usual Yang-Mills Lagrangian. The second part is the potential with the parameter r_0 that is a characteristic length of the model. r_0 is the "size" of the electron, giving the "radius" of our particle. That means inside that radius the potential is high and the field has all SU(2) degrees of freedom. Going to distances $r \gg r_0$ we

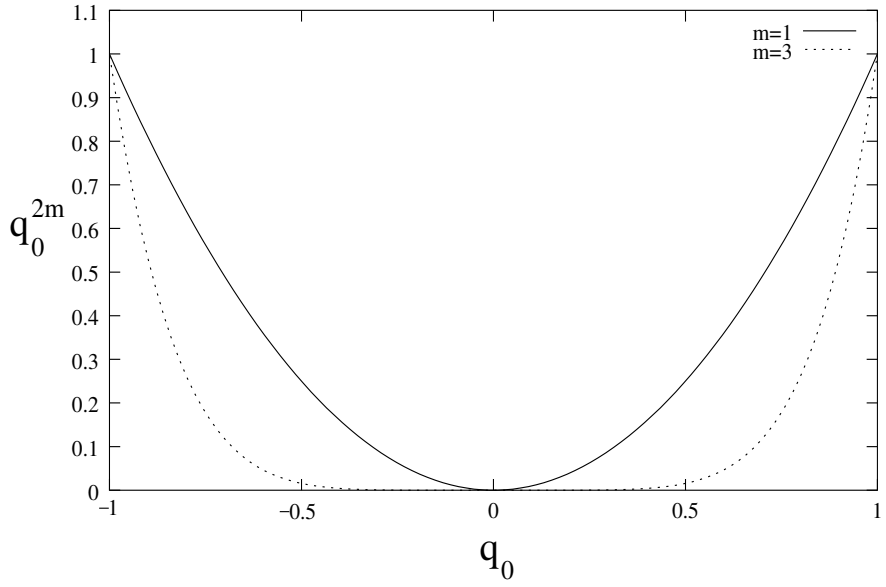

Figure 1.3: Two different potentials. One can see how the potential with m=1 penalizes "high" q_0 more than the one with m=3. Therefore the field in a potential with m=1 will seek to stay mostly at "low" q_0. This leads to a smaller particle.

only observe electrodynamics (see Chapter 2). We also see the parameter m. It gives the power of the confining potential. For large values of m the particle can spread over a bigger area, since the function does not grow so fast (this is true for $0 < q_0 < 1$). See figure (1.3).

Chapter 2

From Soliton Fields to Maxwell's Electromagnetism

So far we have formulated the basic equations of the model. In this chapter we will show how for large distances ($r \gg r_0$) Maxwell's equations can be derived from the topology of the model and a variational principle. We will call the limit for large distances also the electrodynamical limit. Maxwell's equations also come out of the equations of motion of the MTF. Because of the topological structure we expect only electrons as sources of the electromagnetic field. This is the difference to Maxwell's equations that allow arbitrary charge distributions. We also show that after applying a rotation to the soliton field in the region $r \gg r_0$, we get the equivalent of a U(1) gauge theory.

2.1 Where is the Electromagnetism

As mentioned in Chapter 1 the soliton field lives on the S^3. Due to the potential that goes to zero for $r \to \infty$, the soliton field is restricted to the equator of the S^3 for large distances from the center of the soliton. The parameter q_0 in equation (1.3) goes to zero for $r \to \infty$. The only remaining degrees of freedom are on the S^2. That means the only field components relevant at large distances are the $\mathbf{n}$-fields. In the tangent space at large distances we can only define two independent directions. This corresponds to the two transversal components of the photon field. We now take a look at how the connection coefficients and therefore the field strength looks like if we restrict the field to the S^2. If we set $q_0 = 0$ in

$$\mathbf{\Gamma}_\mu = -q_0 \partial_\mu \mathbf{q} + \mathbf{q} \partial_\mu q_0 - \mathbf{q} \times \partial_\mu \mathbf{q} \tag{2.1}$$

we get

$$\mathbf{\Gamma}_\mu = -\mathbf{n} \times \partial_\mu \mathbf{n} \tag{2.2}$$

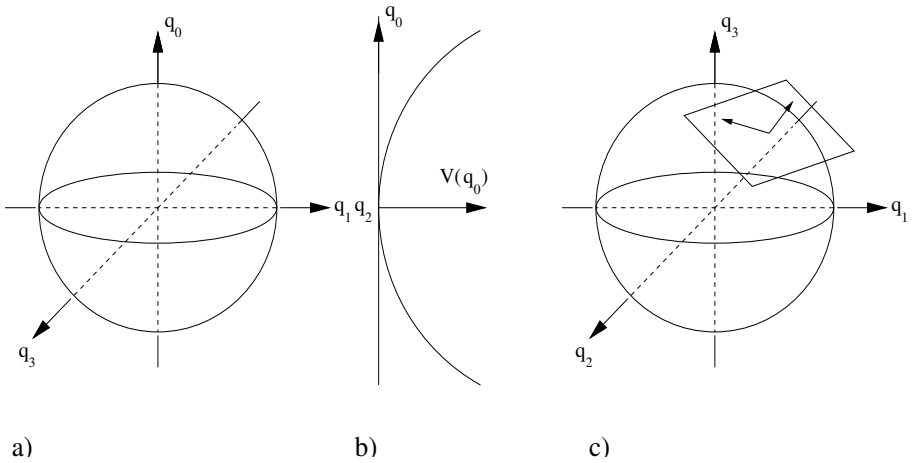

Figure 2.1: The parameter-space of the soliton field. In a) one can see the whole S^3. In b) the potential that limits the field to the S^2 for large distances from the soliton core is shown. c) shows the S^2 with the two remaining degrees of freedom in the tangential plane.

When we insert this into the equation for the field strength we get

$$\mathbf{R}_{\mu\nu} = \mathbf{\Gamma}_\mu \times \mathbf{\Gamma}_\nu = (\mathbf{n} \times \partial_\mu \mathbf{n}) \times (\mathbf{n} \times \partial_\nu \mathbf{n}) \tag{2.3}$$

$$\mathbf{R}_{\mu\nu} = \mathbf{n}(\mathbf{n} \cdot (\partial_\mu \mathbf{n} \times \partial_\nu \mathbf{n})) \tag{2.4}$$

That means the field strength has the direction of $\mathbf{n}$ and the absolute value of $\mathbf{n} \cdot (\partial_\mu \mathbf{n} \times \partial_\mu \mathbf{n})$. How does this field strength relate to the field strength tensor from Maxwell's theory? To clarify things we will look first at the most simple system, the one particle state.

2.2 Solution for one Particle

The solution for a single electron is stated in [2] and is inspired from the hedgehog solution of the Skyrme model. We only state the solution here and have a look at the field strengths calculated from this solution. All we need is the equation for the vector field $\mathbf{n}$. For convenience we use spherical coordinates.

$$\mathbf{n} = \frac{\mathbf{r}}{\sqrt{\mathbf{r}^2 + r_0^2}} = \frac{1}{\sqrt{r^2 + r_0^2}} \begin{pmatrix} r \sin\theta \sin\phi \\ r \sin\theta \cos\phi \\ r \cos\theta \end{pmatrix} \tag{2.5}$$

For large distances from the core this reduces to

$$\mathbf{n} = \begin{pmatrix} \sin\theta \sin\phi \\ \sin\theta \cos\phi \\ \cos\theta \end{pmatrix} \tag{2.6}$$

For the components of the field strength tensor we get

$$\mathbf{R}_{rr} = \mathbf{R}_{\theta\theta} = \mathbf{R}_{\phi\phi} = 0. \tag{2.7}$$

from the antisymmetric vector product. $\mathbf{n}$ does not depend on r. Therefore we get

$$\mathbf{R}_{r\theta} = \mathbf{R}_{r\phi} = \mathbf{R}_{\theta r} = \mathbf{R}_{\phi r} = 0. \tag{2.8}$$

The only remaining component is

$$\mathbf{R}_{\theta\phi} = \frac{1}{r^2}\mathbf{n}. \tag{2.9}$$

This gives the expected Coulomb law, but the entry in the field strength tensor seems to be in the wrong place. It is in the right place, though, if we use the dual formulation of electrodynamics. The vacuum Maxwell equations are dual in the way that one can exchange $\mathbf{B} \leftrightarrow \mathbf{E}$ and $\mathbf{E} \leftrightarrow -\mathbf{B}$ (see e.g. [3]). So we identify

$$F_{\mu\nu} \overset{?}{\leftrightarrow} *\mathbf{R}_{\mu\nu}. \tag{2.10}$$

There seems to remain one problem: The right hand side of equation (2.10) has additional degrees of freedom, coming from the underlying SU(2) field. In order to get U(1) electromagnetism, one has to get rid of these degrees of freedom.

2.2.1 Formulation in SI-Units

As we see in equation (2.9) the usual fore-factor known from electrodynamics missing. If we correct this, we get the dual potential

$$\mathbf{C}_\mu(x) = -\frac{e_0}{4\pi\varepsilon_0}\mathbf{\Gamma}_\mu(x) = \frac{e_0}{4\pi\varepsilon_0}\mathbf{n}(x) \times \partial_\mu \mathbf{n}(x) \tag{2.11}$$

and the dual field strength tensor

$${}^*\mathbf{F}_{\mu\nu}(x) = -\frac{e_0}{4\pi\varepsilon_0 c}\mathbf{R}_{\mu\nu}(x) = -\frac{e_0}{4\pi\varepsilon_0 c}\partial_\mu \mathbf{n}(x) \times \partial_\nu \mathbf{n}(x). \tag{2.12}$$

We can also make a definition for the abelian field strength in SI-units

$$*f_{\mu\nu}(x) = -\frac{e_0}{4\pi\epsilon_0 c}[\partial_\mu \mathbf{n}(x) \times \partial_\nu \mathbf{n}(x)] \cdot \mathbf{n}(x) \tag{2.13}$$

2.3 The Inhomogeneous Maxwell Equations

For the electrodynamical limit the $\mathbf{n}$-field can be seen as a mapping from the $\mathbf{R}^3$ without the origin to an S^2. We have to exclude the origin since there the $\mathbf{n}$-field is not defined[1]. The $\mathbf{R}^n \backslash \{0\}$ is homotopic equivalent to an S^{n-1}. They can be continously

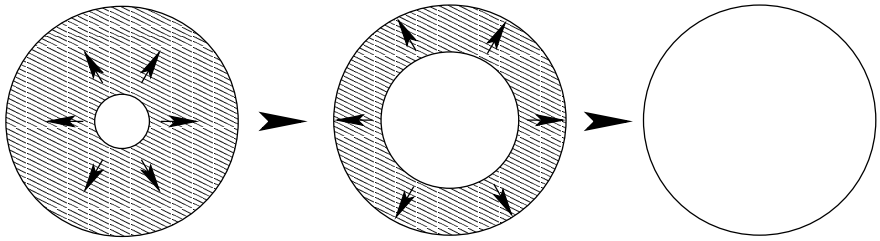

Figure 2.2: The space $\mathbf{R}^n \backslash \{0\}$ in a) is deformed into an S^{n-1} in b). see [4].

deformed into each other (see figure). We know from topology that each homotopy class can be defined by its winding number. In our case we have $\pi_2(S^2) = \mathbf{Z}$. So for every closed surface in $\mathbf{R}^3$ we can assign a charge so that

$$Q = -\mathbf{Z}e_0 \tag{2.14}$$

We can get the winding number from the integral over the curvature tensor

$$\oint_{\partial M} dx^\mu dx^\nu \mathbf{R}_{\mu\nu} \cdot \mathbf{n} = \oint_{\partial M} dx^\mu dx^\nu (\partial_\mu \mathbf{n} \times \partial_\nu \mathbf{n}) \cdot \mathbf{n} = 4\pi \mathbf{Z} \tag{2.15}$$

or using equation (2.13)

$$c \oint_{\partial M} dx^\mu dx^\nu * f_{\mu\nu} = -\frac{\mathbf{Z}e_0}{\epsilon_0} = \frac{Q}{\epsilon_0} \tag{2.16}$$

We can also write this with the charge density $j_0 = \rho c$ as

$$c \oint_{\partial M} dx^\mu dx^\nu * f_{\mu\nu} = -\frac{1}{c\epsilon_0} \int_M dx^1 dx^2 dx^3 j_0 \tag{2.17}$$

The integrand on the LHS of equation (2.17) is just a special case of the dual current three-form

$$*j = \frac{1}{6} \epsilon_{\rho\sigma\nu\mu} dx^\rho dx^\sigma dx^\nu j^\mu \tag{2.18}$$

where we also include electric currents in all three space directions. With $\frac{1}{c^2\epsilon_0} = \mu_0$ we get

$$\oint_{\partial M} *f = -\mu_0 \int_M *j \tag{2.19}$$

Now we use Stokes' theorem in differential geometric notation

$$\int_M d\omega = \oint_{\partial M} \omega \tag{2.20}$$

[1] We encounter this problem only in the electrodynamical limit. In the full theory with an additional degree of freedom we get no singularities or ambiguities at the origin.

We get

$$\int d(*f) = -\mu_0 \int *j \tag{2.21}$$

and after we apply the Hodge operator $*$ to both sides and using $*d* = \delta$ and $**j = j$ we have

$$\delta f = -\mu_0 j \tag{2.22}$$

since we can choose our integration volume arbitrarily. We get the inhomogeneous Maxwell equations in dual form.

2.4 The Homogenous Maxwell Equations Derived from a Variational Principle

Now we want to know about the dynamics of the soliton field, and see how they relate to the Maxwell theory. Therefore we start from the action functional and make a variation. The action in the electrodynamical limit reads

$$S[\mathbf{n}] = -\frac{1}{4}\int d^4x(\mathbf{\Gamma}_\mu \times \mathbf{\Gamma}_\nu)\cdot(\mathbf{\Gamma}^\mu \times \mathbf{\Gamma}^\nu) = -\frac{1}{4}\int d^4x(\partial_\mu \mathbf{n}\times\partial_\nu \mathbf{n})\cdot(\partial^\mu \mathbf{n}\times\partial^\nu \mathbf{n}). \tag{2.23}$$

We have to be careful how we implement the variation. Since the field $\mathbf{n}$ is restricted to the surface of a S^2 not all variations are allowed. A possibility to allow only variations along the sphere is to rotate the vector $\mathbf{n}$ instead of adding a certain amount as usual. So we introduce a varied (rotated) $\mathbf{n}$ by

$$\mathbf{n}' = e^{i\eta\cdot\mathbf{T}}\mathbf{n} \tag{2.24}$$

where the $\mathbf{T}$ are the generators of rotation with $(T_i)_{jk} = -i\epsilon_{ijk}$ and the vector η gives the direction of the rotation.

We want to look for an extremum in the action to give us the equations of motion. At an extremum the first functional derivative vanishes. With our special variation equation (2.24) we can define a functional derivative in the following way

$$\lim_{\epsilon\to 0}\frac{S[e^{i\epsilon\eta\cdot\mathbf{T}}\mathbf{n}] - S[\mathbf{n}]}{\epsilon} = \int d^4x \frac{\delta S[e^{i\epsilon\eta\cdot\mathbf{T}}\mathbf{n}]}{\delta\eta(x)}|_{\eta=0}\eta = 0. \tag{2.25}$$

Since we let ϵ go to zero we can make an expansion in terms of ϵ. The rotated $\mathbf{n}$ is to first order in ϵ

$$e^{i\epsilon\eta\cdot\mathbf{T}}\mathbf{n} = \mathbf{n} + i\epsilon(\eta\cdot\mathbf{T})\mathbf{n} = \mathbf{n} + \epsilon\mathbf{n}\times\eta. \tag{2.26}$$

The derivative of $\mathbf{n}$ becomes

$$\partial_\mu(e^{i\epsilon\eta\cdot\mathbf{T}}\mathbf{n}) = \partial_\mu\mathbf{n} + \epsilon(\partial_\mu\mathbf{n}\times\eta + \mathbf{n}\times\partial_\mu\eta) \tag{2.27}$$

We substitute expression (2.27) in the action functional (2.23). For each $\partial_\mu \mathbf{n}$ we get an additional term $\epsilon(\partial_\mu \mathbf{n} \times \eta + \mathbf{n} \times \partial_\mu \eta)$. We can collect all four terms of this kind in one term since one can always rename the indices which are summed over. For the varied action functional we get

$$S[e^{i\epsilon\eta\cdot\mathbf{T}}\mathbf{n}] = -\frac{1}{4}\int d^4x(\partial^\mu \mathbf{n} \times \partial^\nu \mathbf{n}) \cdot \{[\partial_\mu \mathbf{n} + 4\epsilon(\partial_\mu \mathbf{n} \times \eta + \mathbf{n} \times \partial_\mu \eta)] \times \partial_\nu \mathbf{n}\} \tag{2.28}$$

If we insert (2.23) along with (2.28) in equation (2.25) almost all terms cancel. Also the ϵ in the remaining term cancels with the ϵ in the denominator. Now we can easily take the limit $\epsilon \to 0$ and get

$$\int d^4x[(\partial_\mu \mathbf{n} \times \eta + \mathbf{n} \times \partial_\mu \eta) \times \partial_\nu \mathbf{n}] \cdot (\partial^\mu \mathbf{n} \times \partial^\nu \mathbf{n}) = 0. \tag{2.29}$$

We can rewrite equation (2.29) with the help of some vector identities

$$(\partial_\mu \mathbf{n} \times \eta) \times \partial_\nu \mathbf{n} = \eta(\partial_\mu \mathbf{n} \cdot \partial_\nu \mathbf{n}) - \partial_\mu \mathbf{n}(\eta \cdot \partial_\nu \mathbf{n}) \tag{2.30}$$

and

$$(\mathbf{n} \times \partial_\mu \eta) \times \partial_\nu \mathbf{n} = -\mathbf{n}(\partial_\mu \eta \cdot \partial_\nu \mathbf{n}). \tag{2.31}$$

The second cross product in equation (2.29) is antisymmetric in the indices μ and ν. Therefore the symmetric terms in (2.30) and (2.31) do not contribute and only the second term in (2.30) remains. So we get

$$\int d^4x\, (\partial_\mu \vec{\eta} \cdot \partial_\nu \mathbf{n})\mathbf{n} \cdot (\partial^\mu \mathbf{n} \times \partial^\nu \mathbf{n}) = 0. \tag{2.32}$$

We can rewrite the first term as $\partial_\nu(\partial_\mu \vec{\eta} \cdot \mathbf{n})$ since the other term coming from the differentiation is symmetric in μ and ν and vanishes with the second term in (2.32). Now we make a partial integration, moving the derivative from the first to the second term

$$\int d^4x\, (\partial_\mu \eta \cdot \mathbf{n})\, \partial_\nu[\mathbf{n} \cdot (\partial^\mu \mathbf{n} \times \partial^\nu \mathbf{n})] = 0. \tag{2.33}$$

The field η is an arbitrary field. So we can always choose an η so that the first term is different from zero. The only possibility to make the integral zero is that the second term vanishes. Therefore we get the homogenous Maxwell equations.

$$\partial_\nu[\mathbf{n} \cdot (\partial^\mu \mathbf{n} \times \partial^\nu \mathbf{n})] = \partial_\nu * f^{\mu\nu} = 0. \tag{2.34}$$

2.5 The Homogenous Maxwell Equations Derived from the Equations of Motion

There is another way to get the homogenous Maxwell equations. We start from the equation of motion given in ([2]).

$$\partial_\mu(\mathbf{\Gamma}_\nu \times \mathbf{R}^{\mu\nu}) + \mathbf{q}\frac{d\Lambda}{dq_0} = 0 \tag{2.35}$$

with

$$\Lambda = \frac{1}{r_0^4} q_0^6. \tag{2.36}$$

We can neglect the potential term (equation (2.36)) for $r \gg r_0$. Now we use equation (2.2) and (2.4) in equation (2.35).

$$\partial_\mu((\mathbf{n} \times \partial_\nu \mathbf{n}) \times (\partial^\mu \mathbf{n} \times \partial^\nu \mathbf{n})) = 0 \tag{2.37}$$

Evaluating the cross product we get

$$\partial_\mu(\partial^\nu \mathbf{n}\, \partial^\mu \mathbf{n} \cdot (\partial_\nu \mathbf{n} \times \mathbf{n})) = 0 \tag{2.38}$$

After differentiation and exchanging the variables in the product the equation reads

$$-\partial_\mu\partial_\nu \mathbf{n}\, \mathbf{n} \cdot (\partial^\nu \mathbf{n} \times \partial^\mu \mathbf{n}) + \partial_\nu \mathbf{n}\, \partial_\mu(\partial^\mu \mathbf{n} \cdot (\partial^\nu \mathbf{n} \times \mathbf{n})) = 0 \tag{2.39}$$

The first term vanishes, because the differentiation is symmetric in the Lorentz-indices and the cross-product is antisymmetric. After multiplying the second term with $\mathbf{n}\times$ and using $*f^{\mu\nu} = \mathbf{n} \cdot (\partial^\nu \mathbf{n} \times \partial^\mu \mathbf{n})$ we have

$$(\mathbf{n} \times \partial_\nu \mathbf{n})\, \partial_\mu R^{\mu\nu} = \mathbf{\Gamma}_\nu\, \partial_\mu * f^{\mu\nu} = 0 \tag{2.40}$$

These are almost the homogeneous Maxwell equations. One uncertainty remains. We can make a Lorentz transformation in such a way that either the space-like or the time-like components of the potential $\mathbf{\Gamma}_\nu$ vanish. Then it is possible that either $\partial_\mu * f^{\mu 0} = j^0_M \neq 0$ or $\partial_\mu * f^{\mu i} = j^i_M \neq 0$. This would correspond to a magnetic charge or a magnetic current. But as we will see they are not allowed in the theory. The tensor $R^{\mu\nu}$ is gauge independent, the potential $\mathbf{\Gamma}_\nu$ is not. So we can always make a gauge transformation as introduced on p.14, that changes the components of $\mathbf{\Gamma}_\nu$ in a way that they are not zero. That means we can always find a gauge so that

$$\partial_\mu * f^{\mu\nu} = 0 \tag{2.41}$$

holds.

2.6 The Coupling of a Point Particle to a Soliton Field in the Electrodynamical Limit

We derived that far away from the soliton core the soliton field behaves exactly like an electromagnetic field. But how do the cores enter in to the picture? They behave like point particles with a certain rest mass m_0. In the full model the field far away and the field at the core, that gives the particle most of its mass, are the same. When we take the electrodynamical limit we have to reintroduce this relationship artificially by coupling the $\mathbf{n}$-field to a point particle with rest mass m_0. We will do this by means of coupling the actions of the point particle and of the free electromagnetic field under the constraint that Maxwell's equations must be fulfilled. The mathematically correct way to do this is to introduce Lagrange multipliers (following the discussion in [6]) for the constraint. We will see that we can identify these multipliers with the gauge field. The action for the coupled system reads

$$\begin{aligned} S = & \int d^4x \{ \frac{1}{\mu_0} [-\frac{1}{4} * f_{\mu\nu}(x) * f^{\mu\nu}(x) + a_\nu(x) \partial_\mu f^{\mu\nu}(x)] + \\ & + \int d\tau [e_0 c a_\nu(x) \tfrac{dX^\nu(\tau)}{d\tau} - m_0 c^2 \sqrt{\tfrac{dX_\mu}{d\tau} \tfrac{dX^\mu}{d\tau}}] \delta^4(x - X(\tau)) \} \end{aligned} \tag{2.42}$$

where the first term is the free electromagnetic field, the second term and the third term form the inhomogeneous Maxwell equation, where the current density consists of a point particle moving with a velocity $u^\nu = \frac{dX^\nu(\tau)}{d\tau}$ in its eigenframe. The fourth term is simply the action for a free moving point particle.

We vary now with respect to $\mathbf{n}$ as prescribed in (2.25). To do this we have to express the terms containing $f_{\mu\nu}$ in terms of $\mathbf{n}$. We know that up to a constant factor

$$*f_{\mu\nu}(x) = (\partial_\mu \mathbf{n}(x) \times \partial_\nu \mathbf{n}(x)) \cdot \mathbf{n}(x) \tag{2.43}$$

and for a Minkowskian metric

$$f^{\mu\nu} = *(*f^{\mu\nu}) = -\frac{1}{2} \varepsilon^{\sigma\rho\mu\nu} * f^{\rho\sigma} = -\frac{1}{2} \varepsilon^{\sigma\rho\mu\nu} (\partial_\rho \mathbf{n}(x) \times \partial_\sigma \mathbf{n}(x)) \cdot \mathbf{n}(x) \tag{2.44}$$

Therefore we get for the terms in the action depending on $\mathbf{n}$

$$S_{\mathbf{n}} = \int d^4x \begin{pmatrix} -\frac{1}{4} (\partial_\mu \mathbf{n}(x) \times \partial_\nu \mathbf{n}(x)) \cdot (\partial^\mu \mathbf{n}(x) \times \partial^\nu \mathbf{n}(x)) - \\ -\frac{1}{2} a_\rho \partial_\sigma \varepsilon^{\mu\nu\rho\sigma} (\partial_\mu \mathbf{n}(x) \times \partial_\nu \mathbf{n}(x)) \cdot \mathbf{n}(x) \end{pmatrix} \tag{2.45}$$

where we exchanged $\sigma \leftrightarrow \mu$ and $\rho \leftrightarrow \nu$ in the second term. We already know how to vary the first term. For the variation of the second term we get

$$\int d^4x \left[\frac{1}{2}a_\rho \partial_\sigma \varepsilon^{\mu\nu\rho\sigma} \left((\mathbf{n}\times\eta)\cdot(\partial_\mu \mathbf{n}(x)\times\partial_\nu \mathbf{n}(x)) - \right.\right.$$
$$\left.\left. -2\mathbf{n}\cdot[(\partial_\mu \mathbf{n}\times\eta + \mathbf{n}\times\partial_\mu\eta)\times\partial_\nu \mathbf{n}]\right)] = 0 \tag{2.46}$$

using equations (2.26) and (2.27). The first term vanishes because the two factors are perpendicular. Combining this result with equation (2.29) we get

$$\int d^4x[(\partial_\mu \mathbf{n}\times\eta + \mathbf{n}\times\partial_\mu\eta)\times\partial_\nu \mathbf{n}]\cdot(a_\rho\partial_\sigma\varepsilon^{\mu\nu\rho\sigma}\mathbf{n} + (\partial^\mu \mathbf{n}\times\partial^\nu \mathbf{n})) = 0. \tag{2.47}$$

Using again that the product of terms symmetric and antisymmetric in μ and ν vanish we get

$$\int d^4x(\partial_\mu\eta\cdot\partial_\nu \mathbf{n})\mathbf{n}\cdot(a_\rho\partial_\sigma\varepsilon^{\mu\nu\rho\sigma}\mathbf{n} + (\partial^\mu \mathbf{n}\times\partial^\nu \mathbf{n})) = 0. \tag{2.48}$$

By partial integration we can shift the derivative from $\mathbf{n}$ to a_ρ trading in a minus sign

$$\int d^4x(\partial_\mu\eta\cdot\partial_\nu \mathbf{n})\,(\partial_\sigma a_\rho\varepsilon^{\mu\nu\rho\sigma} - \mathbf{n}\cdot(\partial^\mu \mathbf{n}\times\partial^\nu \mathbf{n})) = 0. \tag{2.49}$$

Since the function η is arbitrary the right expression has to be zero and we get

$$\partial_\sigma a_\rho\varepsilon^{\mu\nu\rho\sigma} - *f^{\mu\nu} = 0. \tag{2.50}$$

Due to the totally antisymmetric ε-tensor we can write $\frac{1}{2}(\partial_\sigma a_\rho - \partial_\rho a_\sigma)$ instead of $\partial_\sigma a_\rho$ and recognizing that

$$\frac{1}{2}(\partial_\sigma a_\rho - \partial_\rho a_\sigma)\varepsilon^{\mu\nu\rho\sigma} = *(\partial^\mu a^\nu - \partial^\nu a^\mu) \tag{2.51}$$

we get the equation for the field strength tensor

$$f_{\mu\nu} = \partial_\mu a_\nu - \partial_\nu a_\mu. \tag{2.52}$$

2.7 Gauging Away the Internal Degrees of Freedom

Now we are going to show that in the limit of large distances ($r \gg r_0$) the U(1) Maxwell electromagnetism follows from our SU(2) theory. We start by introducing a local rotation of the soliton field, corresponding to a gauge-transformation. When we write the connection coefficients in matrix representation, the gauge transformation looks like

$$\Gamma_s \to \Gamma_s' = \Omega(\Gamma_s + i\partial_s)\Omega^\dagger \tag{2.53}$$

2.7.1 A Special Case: One Particle

We can write down the connection coefficients in matrix notation for one particle when we insert equation (2.5) in equation (2.2) and multiply with the generator $\mathbf{T}$. We get

$$\Gamma_r = 0 \qquad \Gamma_\theta = -\mathbf{T}\cdot\mathbf{e}_\phi \qquad \Gamma_\phi = \sin\theta\mathbf{T}\cdot\mathbf{e}_\phi \tag{2.54}$$

Now we want to apply the local rotation in such a way, that only one component remains. So we rotate by the angle θ around the $\mathbf{e}_\phi$-axis. After this rotation all connection coefficients should be oriented in z-direction. The matrix for this rotation is

$$\Omega = e^{i\theta\mathbf{T}\cdot\mathbf{e}_\phi} = e^{i\theta T_\phi} = 1 + i\sin\theta T_\phi + (\cos\theta - 1)T_\phi^2 \tag{2.55}$$

The gauge transformation for Γ_r is

$$\Gamma_r^{'} = i\Omega\partial_r\Omega^\dagger = 0 \tag{2.56}$$

because Ω does not depend on r. The transformation for Γ_θ is also quite simple

$$\Gamma_\theta^{'} = \Omega(\Gamma_\theta + i\partial_\theta)e^{-i\theta T_\phi} = \Omega(\Gamma_\theta - \Gamma_\theta)\Omega^\dagger = 0 \tag{2.57}$$

The calculation for Γ_ϕ is more complicated but also gives a simple result:

$$\Gamma_\phi = (\cos\theta - 1)T_3 \tag{2.58}$$

There remains only one component and this potential corresponds to the vector potential for a Dirac monopole (see e.g.[4]). Since we use the dual formulation of electrodynamics the potential describes an electric monopole sitting at the origin.

2.7.2 The General Case

We saw for one particle that if we apply a local rotation to the connection field we can recover the abelian gauge freedom of an U(1) theory. When the MTF corresponds to Maxwell electromagnetism at large distances $r \gg r_0$ this should be possible for an arbitrary $\mathbf{n}$-field. We introduce a rotation matrix that rotates by an angle ω around the axis $\mathbf{e}_\omega$.

$$\Omega(x) = e^{-i\omega(\mathbf{x})\cdot\mathbf{T}} = e^{-i\omega\mathbf{e}_\omega(x)\cdot\mathbf{T}} \tag{2.59}$$

where we use the same generators as in (2.24). We apply this gauge transformation (rotation matrix) to our $\mathbf{n}$-field.

$$\mathbf{n}' = \Omega\mathbf{n} = (\mathbf{n}\cdot\mathbf{e}_\omega)\mathbf{e}_\omega + \sin\omega\mathbf{e}_\omega\times\mathbf{n} - \cos\omega\mathbf{e}_\omega\times(\mathbf{e}_\omega\times\mathbf{n}) \tag{2.60}$$

We can write the gauge transformation

$$\Gamma_\mu^{'} = \Omega(\Gamma_\mu + i\partial_\mu)\Omega^\dagger \tag{2.61}$$

after the removal of the generators with the formula

$$\mathbf{\Gamma}_\mu = \mathrm{Tr}(\mathbf{T}\Gamma_\mu) \tag{2.62}$$

as

$$\mathbf{\Gamma}'_\mu = \Omega\mathbf{\Gamma}_\mu + \mathbf{\Omega} \tag{2.63}$$

with

$$\mathbf{\Omega} = \frac{1}{2i}\mathrm{Tr}\,(\mathbf{T}\;\partial_\mu\Omega\;\Omega^\dagger) = -\partial_\mu\omega\;\mathbf{e}_\omega - \sin\omega\;\partial_\mu\mathbf{e}_\omega + (\cos\omega - 1)(\mathbf{e}_\omega \times \partial_\mu\mathbf{e}_\omega). \tag{2.64}$$

The connection in the unrotated coordinate system can be written as

$$\mathbf{\Gamma}_\mu = -\mathbf{n} \times \partial_\mu\mathbf{n}. \tag{2.65}$$

In the rotated coordinate system the connection may have an additional component such that

$$\mathbf{\Gamma}'_\mu = -\mathbf{n}' \times \partial_\mu\mathbf{n}' + \mathbf{n}'(\mathbf{n}' \cdot \mathbf{\Gamma}'_\mu) \tag{2.66}$$

This does not change the relation

$$\partial_\mu\mathbf{n}' = i\Gamma'_\mu\mathbf{n}' = -\mathbf{\Gamma}_\mu \times \mathbf{n}' \tag{2.67}$$

Using equation (2.63) we can rewrite this contribution.

$$\mathbf{n}' \cdot \mathbf{\Gamma}'_\mu = \mathbf{n}' \cdot \Omega\mathbf{\Gamma}_\mu + \mathbf{n}' \cdot \mathbf{\Omega} = \mathbf{n} \cdot \mathbf{\Gamma}_\mu + \mathbf{n}' \cdot \mathbf{\Omega} = \mathbf{n}' \cdot \mathbf{\Omega} \tag{2.68}$$

For the transformed connection we get

$$\mathbf{\Gamma}'_\mu = \mathbf{n}' \times \partial_\mu\mathbf{n}' + \mathbf{n}'(\mathbf{n}' \cdot \mathbf{\Omega}) \tag{2.69}$$

With the connection Γ_μ we can define the covariant derivative

$$D_\mu = \partial_\mu - i\Gamma_\mu \tag{2.70}$$

and we can use this to write the curvature tensor as the commutator of the covariant derivatives

$$R_{\mu\nu} = \mathbf{R}_{\mu\nu} \cdot \mathbf{T} = -i(D_\mu D_\nu - D_\nu D_\mu). \tag{2.71}$$

Using the transformation property

$$D'_\mu = \Omega D_\mu \Omega^\dagger \tag{2.72}$$

the field strength transforms also as

$$R'_{\mu\nu} = \Omega R_{\mu\nu}\Omega^\dagger \tag{2.73}$$

where

$$R'_{\mu\nu} = \mathbf{R}_{\mu\nu} \cdot \mathbf{T} = \left(\partial_\nu\mathbf{\Gamma}'_\mu - \partial_\mu\mathbf{\Gamma}'_\nu + \mathbf{\Gamma}'_\nu \times \mathbf{\Gamma}'_\mu\right) \cdot \mathbf{T} \tag{2.74}$$

Let us look at the special rotations that leave the $\mathbf{n}$-field unchanged. For this we have to choose the $\mathbf{n}$-vectors as axis for the rotation. If we put this into equation (2.63) and use

$$\Omega\mathbf{\Gamma}_\mu = \sin\omega(\mathbf{n}\times\mathbf{\Gamma}_\mu) - \cos\omega(\mathbf{n}\times(\mathbf{n}\times\mathbf{\Gamma}_\mu)) = \sin\omega\partial_\mu\mathbf{n} - \cos\omega(\mathbf{n}\times\partial_\mu\mathbf{n}) \quad (2.75)$$

we get for the gauge transformation

$$\mathbf{\Gamma}'_\mu = \mathbf{\Gamma}_\mu - \partial_\mu\omega\mathbf{n}. \quad (2.76)$$

We see that this is the same relation as for U(1) electrodynamics. So all rotations around the $\mathbf{n}$-vectors correspond to a U(1) gauge-transformation.

For the one-particle case we turned everything in 3-direction and got the results for dual electrodynamics. So let us apply a rotation matrix that rotates every $\mathbf{n}$-vector in 3-direction. The matrix to do this is

$$\Omega(x) = e^{-i\theta(x)\mathbf{e}_\phi(x)\cdot\mathbf{T}} \quad (2.77)$$

and the $\mathbf{n}$-field looks like

$$\mathbf{n}' = \Omega\mathbf{n} = \begin{pmatrix} 0 \\ 0 \\ 1 \end{pmatrix} = \mathbf{e}_3 \quad (2.78)$$

where we set

$$\omega = -\theta \text{ and } \mathbf{e}_\omega = \mathbf{e}_\phi = \cos\phi\mathbf{e}_2 - \sin\phi\mathbf{e}_1 \quad (2.79)$$

If we substitute this in (2.69) we can calculate

$$\mathbf{\Gamma}'_\mu = \mathbf{e}_3(\mathbf{e}_3\cdot\mathbf{\Omega}) \quad (2.80)$$

with

$$\mathbf{\Omega} = \partial_\mu\theta\mathbf{e}_\phi + \sin\theta\partial_\mu\mathbf{e}_\phi + (\cos\theta - 1)(\mathbf{e}_\phi\times\partial_\mu\mathbf{e}_\phi). \quad (2.81)$$

We use

$$\partial_\mu\mathbf{e}_\phi = -(\sin\phi\mathbf{e}_2 + \cos\phi\mathbf{e}_1)\partial_\mu\phi. \quad (2.82)$$

Since we need only the projection of $\mathbf{\Omega}$ on $\mathbf{e}_3$ and the first terms in (3.30) have only components in $\mathbf{e}_1$ and $\mathbf{e}_2$ we can throw them away. We also need only the 3-component of the cross product. We get a simpler equation now:

$$\mathbf{\Gamma}'_\mu = (\cos\theta - 1)(\sin^2\phi + \cos^2\phi)\partial_\mu\phi\mathbf{e}_3 = (\cos\theta - 1)\partial_\mu\phi\mathbf{e}_3. \quad (2.83)$$

After the transformation the curvature becomes

$$\mathbf{R}_{\mu\nu} = \partial_\nu\mathbf{\Gamma}'_\mu - \partial_\mu\mathbf{\Gamma}'_\nu = (\partial_\mu\theta\partial_\nu\phi - \partial_\nu\theta\partial_\mu\phi)\mathbf{e}_3. \quad (2.84)$$

The cross product in (2.74) does not contribute since the connections $\mathbf{\Gamma}_\mu$ and $\mathbf{\Gamma}_\nu$ both point in the direction of $\mathbf{e}_3$ according to (3.29).

For a axially symmetric $\mathbf{n}$-field it is now very easy to calculate the $\mathbf{n}$-field from the electromagnetic vector potential. We will use this on p.26.

Chapter 3

The Two Particle System

In this chapter we look at the interaction of two particles. We discuss how the soliton fields must look like and what symmetries they obey. There are two possible configurations: either the particle-particle interaction or the particle-antiparticle interaction.

3.1 Possible One Particle States

A global rotation of the $\mathbf{n}$-vectors doesn't change the system's energy. Therefore there are an infinite number of equivalent one particle states. We are interested in two different configurations: The unrotated hedgehog solution and the hedgehog solution rotated around a coordinate axis (let's say the x-axis) by 180° (see figure 3.1). There is a further possibility to construct a one particle state. If we look at the S^3 we can construct a state where we start at the north pole and cover the top half of the sphere. We can also construct a state where we start at the south pole and cover the bottom half of the sphere. We can think of it in terms of the parameter q_0. In the first case we start from $q_0 = 1$ and go to $q_0 = 0$. In the second case we start from $q_0 = -1$ and go to the equator with $q_0 = 0$. Both states are physically equivalent because all physically relevant values carry even powers of q_0. In the one particle state they are indistinguishable.

3.2 Fitting the Fields Together

Now we investigate what the two-electron field might look like. If we do it naively and we put two type a) solutions (see Figure 3.1) together, we see that the vectors in the symmetry xy-plane look in different directions. This means that in this plane the derivative is very high and therefore also the field energy. Since the stable solution is the one with the lowest energy this configuration is unfavorable. Now we take a type a) solution at the top and a type b) solution at the bottom. We see the solutions fit much better in the xy-plane. There is only a small adjustment needed to form a smooth transition between the two single-electron solutions. This is the configuration with the lower energy and therefore a candidate for our solution.

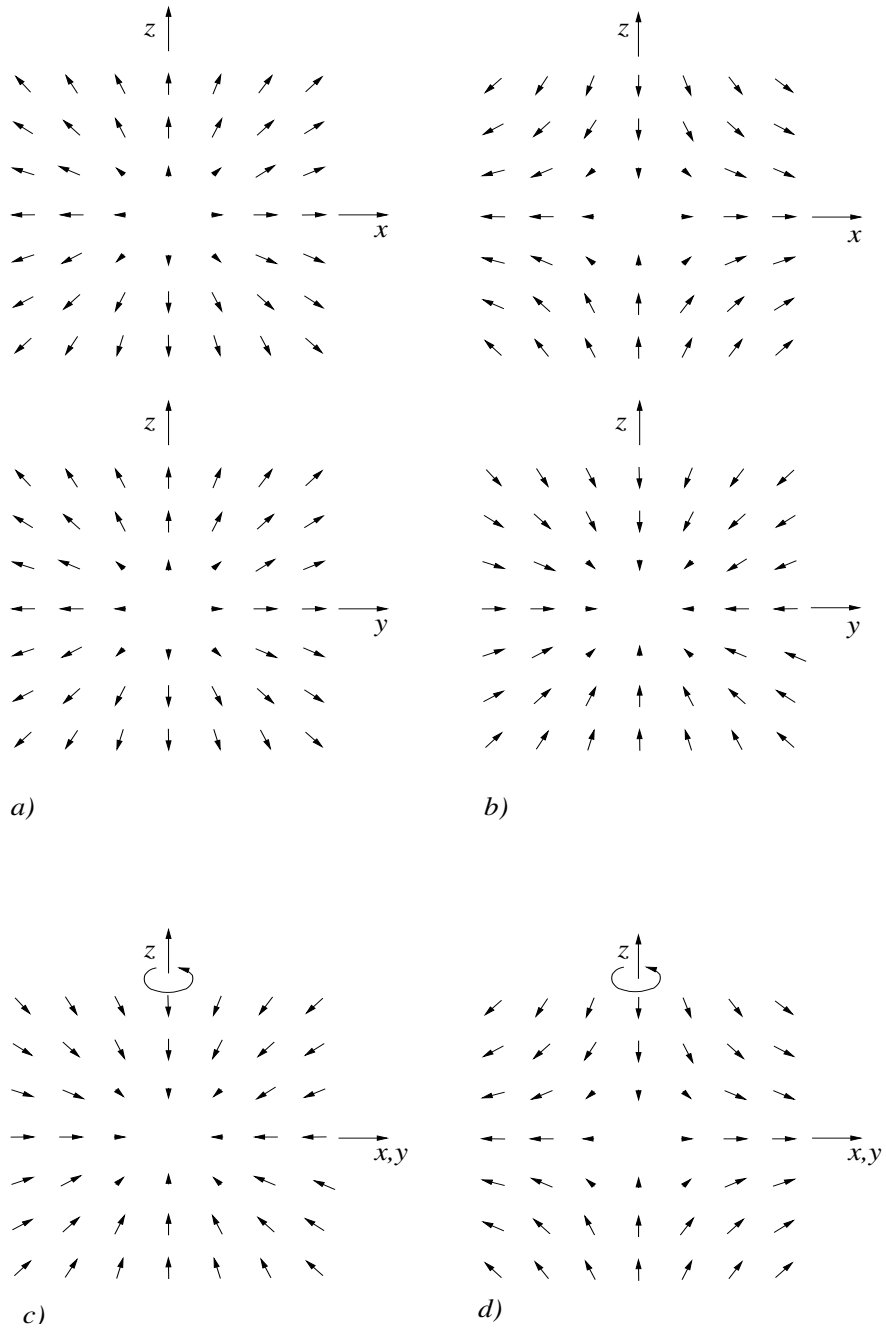

Figure 3.1: The xz-plane and the yz-plane of two different field configurations for the electron. a) is the unrotated hedgehog, b) is rotated 180° about the x-axis. c) is the unrotated hedgehog solution for the positron. d) shows the positron solution type c) rotated 180° about the z-axis.

For the electron-positron field we use similar arguments. When we fit the unrotated electron and the unrotated positron we get an axially symmetric solution as shown in

figure (3.2) a). But this is not the minimum energy solution. The "bulge" in the middle means high derivatives and therefore a high curvature energy. When we rotate the positron solution 180° about the z-axis we get a type d) solution. This fits quite nicely with the electron type a) eliminating the "bulge" and is axially symmetric, too.

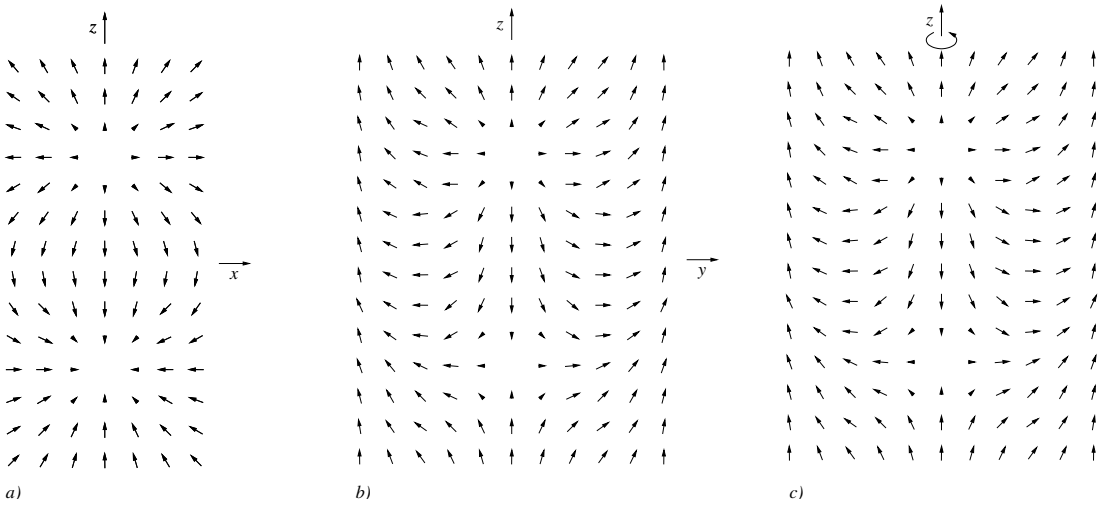

Figure 3.2: a) shows the xz-plane for an electron-electron configuration b) shows the yz-plane for an electron-electron configuration. c) shows the rotational symmetric positron-electron configuration

3.3 Topologically Different States

When we construct two particle states we have to keep the two different one particle states starting at $q_0 = \pm 1$ in mind. There are now two ways to fit single particle states together. We can take a pair with different starting values of q_0 or with equal values. There will be an energy difference between the two configurations (see figure 3.5).

3.4 The Electron-Positron System

3.4.1 Energy Densities for the Electron Positron System

The electron positron-system is axially symmetric. Therefore we can make an ansatz obeying this symmetry.

$$\mathbf{q} = \begin{pmatrix} q_r(r,z)\cos\phi \\ q_r(r,z)\sin\phi \\ q_z(r,z) \end{pmatrix} \tag{3.1}$$

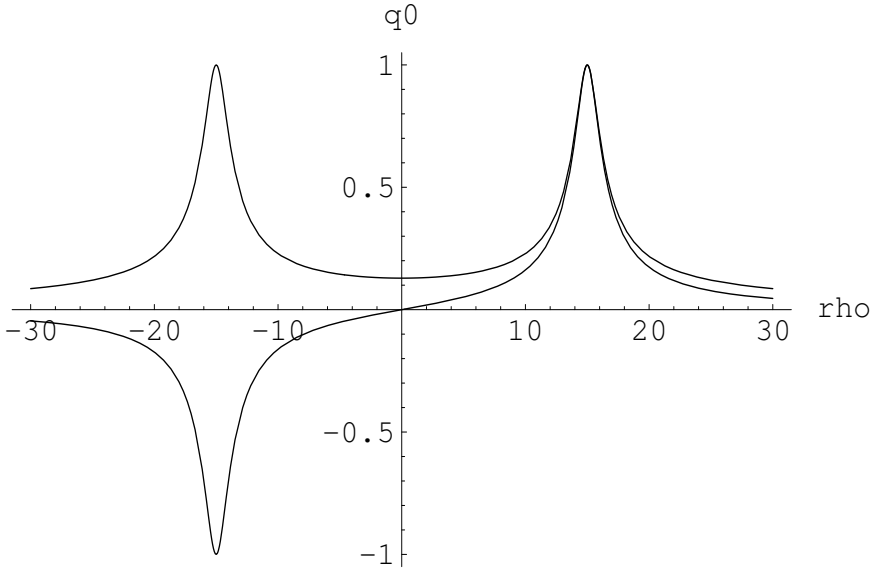

Figure 3.3: Fitting two different one particle solutions together. Both particles sit along the z-axis at z=± 15. Shown is the parameter q_0 as a function of the z-coordinate. We can see the two different possibilities. The distance is given in $\rho = r/r_0$. When we identify the center of the second particle with the south pole of the S^3, q_0 has to pass the equator in order to reach it. Therefore q_0 reaches zero. If both centers lie on the same pole of the S^3 the parameter q_0 goes from one maximum to the other without reaching zero. When the distance between the particles goes to infinity the energy difference between the two states will go to zero.

For the component q_0 we use equation (1.2) and get

$$q_0 = \sqrt{1 - q_r^2 - q_z^2} \tag{3.2}$$

We can plug this in the definition of the connection coefficients

$$\mathbf{\Gamma}_\mu = -q_0 \partial_\mu \mathbf{q} + \mathbf{q} \partial_\mu q_0 - \mathbf{q} \times \partial_\mu \mathbf{q} \tag{3.3}$$

We use cylindrical coordinates. This gives some rather lengthy expressions for the three connection coefficients

$$\mathbf{\Gamma}_\phi = \frac{1}{r} \begin{pmatrix} \cos\phi q_r q_z - \sin\phi q_r q_0 \\ \cos\phi q_r q_0 + \sin\phi q_r q_z \\ -q_r^2 \end{pmatrix} \tag{3.4}$$

$$\mathbf{\Gamma}_r = \frac{1}{q_0} \begin{pmatrix} \cos\phi \left(q_0^2 \frac{\partial q_r}{\partial r} + q_r \left(q_r \frac{\partial q_r}{\partial r} + q_z \frac{\partial q_z}{\partial r} \right) \right) + \sin\phi q_0 \left(q_z \frac{\partial q_r}{\partial r} - q_r \frac{\partial q_z}{\partial r} \right) \\ \sin\phi \left(q_0^2 \frac{\partial q_r}{\partial r} + q_r \left(q_r \frac{\partial q_r}{\partial r} + q_z \frac{\partial q_z}{\partial r} \right) \right) - \cos\phi q_0 \left(q_z \frac{\partial q_r}{\partial r} - q_r \frac{\partial q_z}{\partial r} \right) \\ q_r q_z \frac{\partial q_r}{\partial r} + (1 - q_r^2) \frac{\partial q_z}{\partial r} \end{pmatrix} \tag{3.5}$$

$$\mathbf{\Gamma}_z = \frac{1}{q_0}\begin{pmatrix} \cos\phi\left(q_0^2\frac{\partial q_r}{\partial z} + q_r\left(q_r\frac{\partial q_r}{\partial z} + q_z\frac{\partial q_z}{\partial z}\right)\right) + \sin\phi q_0\left(q_z\frac{\partial q_r}{\partial z} - q_r\frac{\partial q_z}{\partial z}\right) \\ \sin\phi\left(q_0^2\frac{\partial q_r}{\partial z} + q_r\left(q_r\frac{\partial q_r}{\partial z} + q_z\frac{\partial q_z}{\partial z}\right)\right) - \cos\phi q_0\left(q_z\frac{\partial q_r}{\partial z} - q_r\frac{\partial q_z}{\partial z}\right) \\ q_r q_z\frac{\partial q_r}{\partial z} + (1-q_r^2)\frac{\partial q_z}{\partial z} \end{pmatrix} \tag{3.6}$$

with q_0 as defined in equation (3.2). Now we can use this to calculate the curvature part of the energy density.

$$\mathcal{H}_c = \frac{1}{4}\mathbf{R}_{\mu\nu}\cdot\mathbf{R}^{\mu\nu} \tag{3.7}$$

where only the off-diagonal elements contribute. Therefore we get

$$\mathcal{H}_c = \frac{1}{4}\left(\mathbf{R}_{rz}\cdot\mathbf{R}_{rz} + \mathbf{R}_{\phi z}\cdot\mathbf{R}_{\phi z} + \mathbf{R}_{r\phi}\cdot\mathbf{R}_{r\phi}\right) \tag{3.8}$$

Using

$$\mathbf{R}_{\mu\nu} = \mathbf{\Gamma}_\mu \times \mathbf{\Gamma}_\nu \tag{3.9}$$

we can write down the three elements of the field strength tensor.

$$\mathbf{R}_{rz} = \frac{\frac{\partial q_z}{\partial z}\frac{\partial q_r}{\partial r} - \frac{\partial q_z}{\partial r}\frac{\partial q_r}{\partial z}}{\sqrt{1-q_r^2-q_z^2}}\begin{pmatrix} -q_z\cos\varphi + \sqrt{1-q_r^2-q_z^2}\sin\varphi \\ -q_z\sin\varphi - \sqrt{1-q_r^2-q_z^2}\cos\varphi \\ q_r \end{pmatrix} \tag{3.10}$$

$$\mathbf{R}_{rp} = \frac{q_r}{\sqrt{1-q_r^2-q_z^2}}\begin{pmatrix} \left(q_r\frac{\partial q_r}{\partial r} + q_z\frac{\partial q_z}{\partial r}\right)\sin\varphi + \sqrt{1-q_r^2-q_z^2}\frac{\partial q_z}{\partial r}\cos\varphi \\ \left(q_r\frac{\partial q_r}{\partial r} + q_z\frac{\partial q_z}{\partial r}\right)\cos\varphi - \sqrt{1-q_r^2-q_z^2}\frac{\partial q_z}{\partial r}\sin\varphi \\ \frac{\partial q_r}{\partial r}\sqrt{1-q_r^2-q_z^2} \end{pmatrix} \tag{3.11}$$

$$\mathbf{R}_{zp} = \frac{q_r}{\sqrt{1-q_r^2-q_z^2}}\begin{pmatrix} \left(q_r\frac{\partial q_r}{\partial z} + q_z\frac{\partial q_z}{\partial z}\right)\sin\varphi + \sqrt{1-q_r^2-q_z^2}\frac{\partial q_z}{\partial z}\cos\varphi \\ \left(q_r\frac{\partial q_r}{\partial z} + q_z\frac{\partial q_z}{\partial z}\right)\cos\varphi - \sqrt{1-q_r^2-q_z^2}\frac{\partial q_z}{\partial z}\sin\varphi \\ \frac{\partial q_r}{\partial z}\sqrt{1-q_r^2-q_z^2} \end{pmatrix} \tag{3.12}$$

and for the contributions to the energy density (3.8)

$$\mathbf{R}_{rz}\cdot\mathbf{R}_{rz} = \frac{1}{1-q_r^2-q_z^2}\left(\frac{\partial q_z}{\partial z}\frac{\partial q_r}{\partial r} - \frac{\partial q_z}{\partial r}\frac{\partial q_r}{\partial z}\right)^2 \tag{3.13}$$

$$\mathbf{R}_{rp}\cdot\mathbf{R}_{rp} = \frac{q_r^2}{r^2\left(1-q_r^2-q_z^2\right)}\left(\left(q_r\frac{\partial q_r}{\partial r} - q_z\frac{\partial q_z}{\partial r}\right)^2 - \left(\frac{\partial q_r}{\partial r}\right)^2 - \left(\frac{\partial q_z}{\partial r}\right)^2\right) \tag{3.14}$$

$$\mathbf{R}_{zp} \cdot \mathbf{R}_{zp} = \frac{q_r^2}{r^2\left(1-q_r^2-q_z^2\right)}\left(\left(q_r\frac{\partial q_r}{\partial z} - q_z\frac{\partial q_z}{\partial z}\right)^2 - \left(\frac{\partial q_r}{\partial z}\right)^2 - \left(\frac{\partial q_z}{\partial z}\right)^2\right) \quad (3.15)$$

We finally get for the energy density

$$\begin{aligned}\mathcal{H}_c = \frac{1}{4}\frac{1}{r^2\sqrt{q_r^2+q_z^2-1}}\Bigg(-r^2\left(\frac{\partial q_z}{\partial z}\frac{\partial q_r}{\partial r} - \frac{\partial q_z}{\partial r}\frac{\partial q_r}{\partial z}\right)^2 - \\ -2q_r^3 q_z\left(\tfrac{\partial q_r}{\partial z}\tfrac{\partial q_z}{\partial z} + \tfrac{\partial q_r}{\partial r}\tfrac{\partial q_z}{\partial r}\right) + q_r^4\left(\left(\tfrac{\partial q_z}{\partial z}\right)^2 + \left(\tfrac{\partial q_z}{\partial r}\right)^2\right) + \\ +q_r^2\left(\left(q_z^2-1\right)\left(\left(\tfrac{\partial q_r}{\partial z}\right)^2 + \left(\tfrac{\partial q_r}{\partial r}\right)^2\right) - \left(\tfrac{\partial q_z}{\partial z}\right)^2 - \left(\tfrac{\partial q_z}{\partial r}\right)^2\right)\Bigg)\end{aligned} \quad (3.16)$$

As expected there is no more ϕ dependence in the final expression. Now we have reduced the three dimensional problem to a two dimensional one. One problem remains. The expression seems to have a singularity at the origin. We know this comes from the $\mathbf{\Gamma}_\phi$ part. We also know the ϕ-direction does not make any sense in the origin. To get a non-singular expression for the energy in the origin we do several things. First we fix our ϕ-direction in the origin. We choose $\phi = 0$. For the $\mathbf{\Gamma}_\phi$ we make the following substitution. In cylindrical coordinates the ϕ-direction is always perpendicular to the r-direction. So we also choose a direction in the origin perpendicular to our fixed r-direction to be our ϕ-direction in the origin. This would be the r-direction for $\phi = \pi/2$ (see figure (3.4)). Now we can write down the connections in the origin.

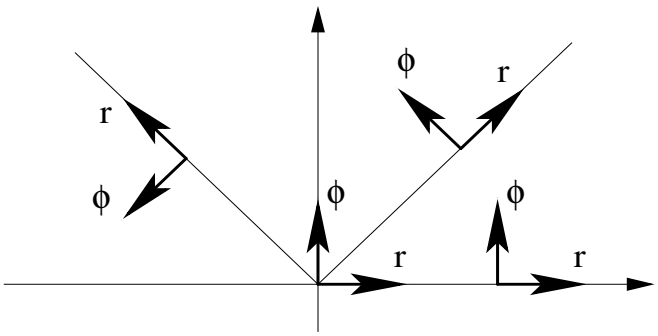

Figure 3.4: Here we see different coordinate frames at different points. We choose a fixed coordinate frame in the origin, as you can see above.

$$\mathbf{\Gamma}_\phi = \frac{1}{q_0}\begin{pmatrix} q_0\left(q_z\frac{\partial q_r}{\partial r} - q_r\frac{\partial q_z}{\partial r}\right) \\ q_0^2\frac{\partial q_r}{\partial r} + q_r\left(q_r\frac{\partial q_r}{\partial r} + q_z\frac{\partial q_z}{\partial r}\right) \\ q_r q_z\frac{\partial q_r}{\partial r} + \left(1-q_r^2\right)\frac{\partial q_z}{\partial r}\end{pmatrix} \quad (3.17)$$

$$\mathbf{\Gamma}_r = \frac{1}{q_0}\begin{pmatrix} q_0^2\frac{\partial q_r}{\partial r} + q_r\left(q_r\frac{\partial q_r}{\partial r} + q_z\frac{\partial q_z}{\partial r}\right) \\ -q_0\left(q_z\frac{\partial q_r}{\partial r} - q_r\frac{\partial q_z}{\partial r}\right) \\ q_r q_z\frac{\partial q_r}{\partial r} + (1-q_r^2)\frac{\partial q_z}{\partial r} \end{pmatrix} \tag{3.18}$$

$$\mathbf{\Gamma}_z = \frac{1}{q_0}\begin{pmatrix} q_0^2\frac{\partial q_r}{\partial z} + q_r\left(q_r\frac{\partial q_r}{\partial z} + q_z\frac{\partial q_z}{\partial z}\right) \\ -q_0\left(q_z\frac{\partial q_r}{\partial z} - q_r\frac{\partial q_z}{\partial z}\right) \\ q_r q_z\frac{\partial q_r}{\partial z} + (1-q_r^2)\frac{\partial q_z}{\partial z} \end{pmatrix}. \tag{3.19}$$

For symmetry reasons the component q_r has to be zero for $r = 0$ and so we can simplify the connections a little further.

$$\mathbf{\Gamma}_\phi = \frac{1}{q_0}\begin{pmatrix} q_0 q_z\frac{\partial q_r}{\partial r} \\ q_0^2\frac{\partial q_r}{\partial r} \\ \frac{\partial q_z}{\partial r} \end{pmatrix} \tag{3.20}$$

$$\mathbf{\Gamma}_r = \frac{1}{q_0}\begin{pmatrix} q_0^2\frac{\partial q_r}{\partial r} \\ -q_0 q_z\frac{\partial q_r}{\partial r} \\ \frac{\partial q_z}{\partial r} \end{pmatrix} \tag{3.21}$$

$$\mathbf{\Gamma}_z = \frac{1}{q_0}\begin{pmatrix} q_0^2\frac{\partial q_r}{\partial z} \\ -q_0 q_z\frac{\partial q_r}{\partial z} \\ \frac{\partial q_z}{\partial z} \end{pmatrix}. \tag{3.22}$$

The energy density becomes

$$\begin{aligned}\mathcal{H}_c = \frac{1}{4}\frac{1}{q_z^2-1}\Bigg[2\frac{\partial q_r}{\partial r}\frac{\partial q_r}{\partial z}\frac{\partial q_z}{\partial r}\frac{\partial q_z}{\partial z} - 2\left(\left(\frac{\partial q_r}{\partial z}\right)^2 + \left(\frac{\partial q_r}{\partial r}\right)^2\right)\left(\frac{\partial q_z}{\partial r}\right)^2 + \\ + \left(\tfrac{\partial q_r}{\partial r}\right)^2\left((q_z^2-1)\left(\left(\tfrac{\partial q_r}{\partial z}\right)^2 + \left(\tfrac{\partial q_r}{\partial r}\right)^2\right) - 2\left(\tfrac{\partial q_z}{\partial z}\right)^2\right)\Bigg]\end{aligned} \tag{3.23}$$

Both expressions are singular for $q_r^2 + q_z^2 \to 1$, that means in the limit of electrodynamics. One can redo the calculation with $q_0 = 0$ and gets for the energy density in the region $r > 0$

$$\mathcal{H}_c = \frac{1}{4}\frac{q_r^2}{r^2}\left(\left(q_z\frac{\partial q_r}{\partial z} - q_r\frac{\partial q_z}{\partial z}\right)^2 + \left(q_z\frac{\partial q_r}{\partial r} - q_r\frac{\partial q_z}{\partial r}\right)^2\right) \tag{3.24}$$

and in the case $r = 0$

$$\mathcal{H}_c = \frac{1}{4}\left(q_z^2\frac{\partial q_r}{\partial r}\right)^2\left(\left(\frac{\partial q_r}{\partial z}\right)^2 + \left(\frac{\partial q_r}{\partial r}\right)^2\right) \tag{3.25}$$

Now one can minimize this energy densities in a computer program and obtain the quasi-static solution for a certain distance between the particles.

3.4.2 Electric Field from an Axially Symmetric Soliton Field

One can also calculate the electric field from an axially symmetric soliton field configuration. In the limit $q_0 \to 0$ at $r \gg r_0$ we get using (2.4)

$$E_z = -\frac{e_0}{4\pi\epsilon_0 c}\frac{q_r}{r}\left(q_z\frac{\partial q_r}{\partial r} - q_r\frac{\partial q_z}{\partial r}\right) \tag{3.26}$$

$$E_r = -\frac{e_0}{4\pi\epsilon_0 c}\frac{q_r}{r}\left(q_z\frac{\partial q_r}{\partial z} - q_r\frac{\partial q_z}{\partial z}\right) \tag{3.27}$$

$$E_\varphi = 0 \tag{3.28}$$

We see that from an axially symmetric soliton field we get an axially symmetric E-field.

3.4.3 The $\mathbf{n}$-field at large distances $r \gg r_0$ calculated from the dual potential

We can now use the result we have obtained on p. 18 and calculate the $\mathbf{n}$-field of an electron-positron pair. We can use the axial symmetry. Let us look at the formula for the vector potential.

$$\mathbf{\Gamma}_\mu = (\cos\theta - 1)\partial_\mu\phi\mathbf{e}_3. \tag{3.29}$$

ϕ and θ denote the "internal" coordinates, the angles of the $\mathbf{n}$-field. When we identify the internal angle ϕ with the external angle φ, we get just one contribution from the potential

$$\Gamma_\varphi = (\cos\theta - 1)\partial_\varphi\varphi = (\cos\theta - 1) \tag{3.30}$$

Now we have to calculate the dual potential. It is the sum of the monopoles, one positive and one negative, sitting at the distance $\pm d$ from the origin at the z-axis as shown in figure (3.5). The potential for one monopole is

$$C_\mu = \frac{\cos\vartheta - 1}{R\sin\vartheta} \tag{3.31}$$

Now we put two monopoles together and use the definitions $z_+ = z+d$ and $z_- = z-d$. For the joint potential we get

$$C_\mu = \frac{\cos\vartheta_+ - 1}{R\sin\vartheta_+} - \frac{\cos\vartheta_- - 1}{R\sin\vartheta_-}. \tag{3.32}$$

Using

$$\cos\vartheta_\pm = \frac{r}{\sqrt{r^2 + z_\pm^2}} \qquad \sin\vartheta_\pm = \frac{z_\pm}{\sqrt{r^2 + z_\pm^2}} \tag{3.33}$$

in the equation above we get

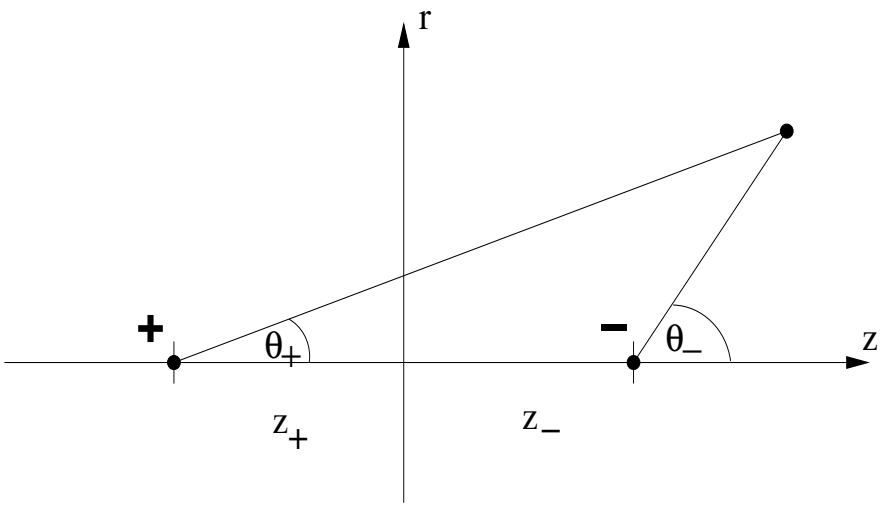

Figure 3.5: The position of the two monopoles with their respective azimuth angles θ_+ and θ_-.

$$C_\mu = \frac{1}{r}\left(\frac{z_+ - \sqrt{r^2+z_+^2}}{\sqrt{r^2+z_+^2}} - \frac{z_- - \sqrt{r^2+z_-^2}}{\sqrt{r^2+z_-^2}}\right) \tag{3.34}$$

In order to get the potential Γ_μ we have to multiply with the line element $R\sin\vartheta$. Therefore we get

$$\Gamma_\mu = \frac{z_+ - \sqrt{r^2+z_+^2}}{\sqrt{r^2+z_+^2}} - \frac{z_- - \sqrt{r^2+z_-^2}}{\sqrt{r^2+z_-^2}} \tag{3.35}$$

and for the azimuth angle subsequently

$$\theta = \arccos\left(\frac{z_+ - \sqrt{r^2+z_+^2}}{\sqrt{r^2+z_+^2}} - \frac{z_- - \sqrt{r^2+z_-^2}}{\sqrt{r^2+z_-^2}} + 1\right) \tag{3.36}$$

We now can write down the $\mathbf{n}$-field quite easily

$$\mathbf{n} = \begin{pmatrix} \cos\varphi\sin\theta \\ \sin\varphi\sin\theta \\ \cos\theta \end{pmatrix} \tag{3.37}$$

The plot of the vector field is shown in figure (3.6). Let us look at some special cases. First we consider the field at $r = 0$. There we get

$$\cos\theta = \frac{z+d-|z+d|}{|z+d|} - \frac{z-d-|z-d|}{|z-d|} + 1 \tag{3.38}$$

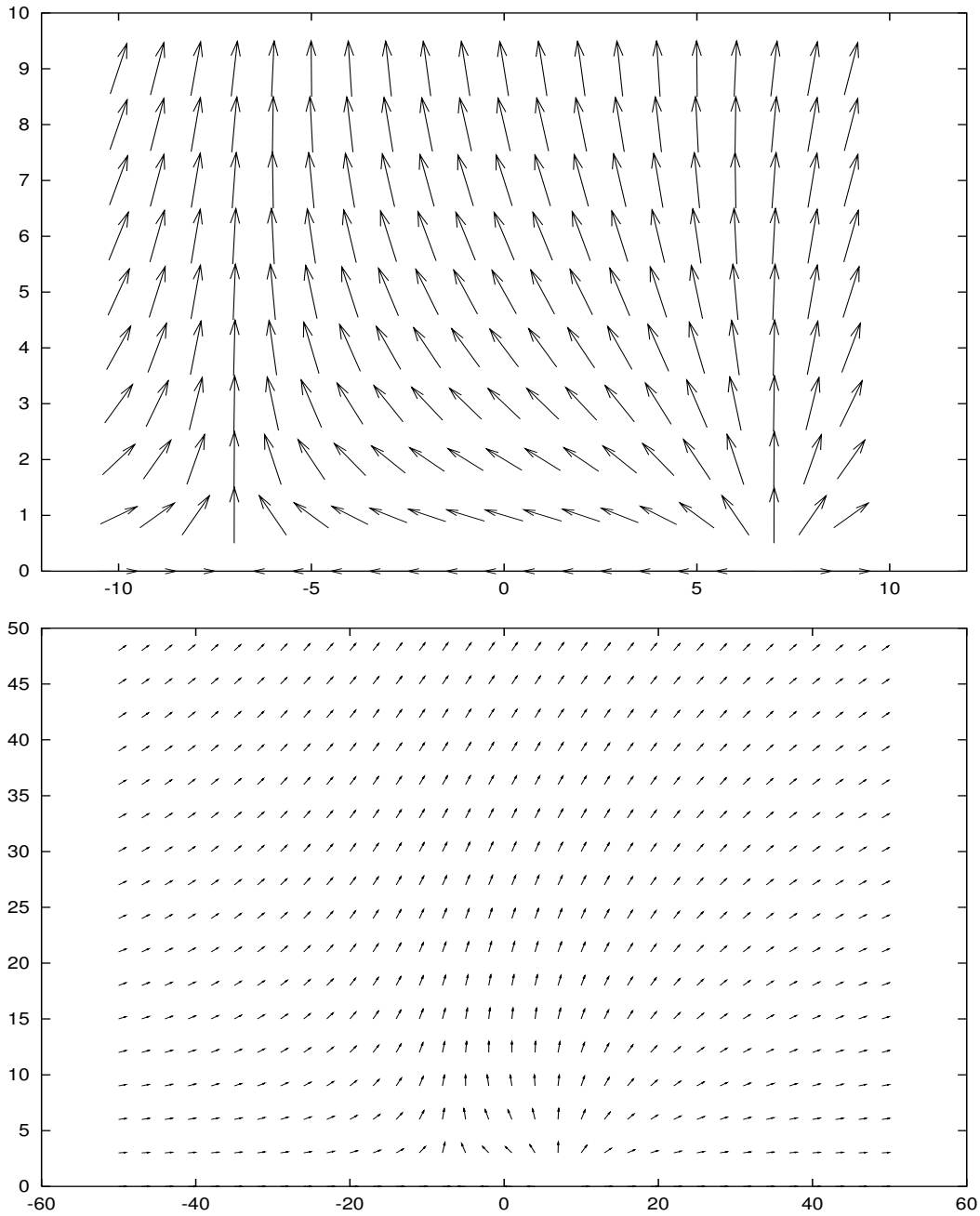

Figure 3.6: The resulting $\mathbf{n}$-field for an electron-positron pair on a lattice with arbitrary units. Two different magnifications of the field configuration are shown. The particles sit at a distance d=15 symmetric to the origin. One can see, that the field only twists right and left from the z-direction, but does not make a whole turn. This indicates that the whole system is uncharged. For large distances from the charges all the arrows align in z-direction. There is no field at infinity.

We have to distinguish three cases. For $z > d$ and $z < -d$ we get $\cos\theta = 1$ and therefore

$$\mathbf{n} = \begin{pmatrix} 0 \\ 0 \\ 1 \end{pmatrix}. \tag{3.39}$$

For $-d < z < d$ we get $\cos\theta = -1$ and therefore

$$\mathbf{n} = \begin{pmatrix} 0 \\ 0 \\ -1 \end{pmatrix}. \tag{3.40}$$

What happens at $z = 0$ when we let $r \to \infty$? Then the field should also point in the positive z-direction. We get

$$\cos\theta = \frac{d_+ - \sqrt{r^2 + d^2}}{\sqrt{r^2 + d^2}} - \frac{-d - \sqrt{r^2 + d^2}}{\sqrt{r^2 + d^2}} + 1. \tag{3.41}$$

In the limit $r \to \infty$ the two first terms cancel each other and the $\mathbf{n}$-field looks like equation (3.39) again.

Chapter 4

Numerical Calculations

Unfortunately it is almost impossible to solve the differential equations analytically for the two-particle system. Therefore we decided to approach the problem by searching a minimum of the Lagrangian numerically. The full electron-electron scattering is a dynamical process, the fields depend on time. This would result in a four-dimensional lattice and an explosion in computing time and use of memory. Therefore we decided to look at "static" solutions, meaning snapshots of the scattering process, where we fix the position of the soliton cores and search for a minimum of the Hamiltonian instead of the Lagrangian.

We do this by solving the problem on a lattice. At each lattice point sits a vector representing the soliton field characterized by a number of parameters depending on the dimensionality of the problem. Derivatives are calculated as differences between the lattice points. Using the derivatives we can calculate the energy density at a given point. The energy density is integrated over the whole lattice. What we get is the energy in the system as a function of the parameters at each point. This function can be minimized with a ready made routine. After a certain number of iterations we get as a result the minimum energy solution obeying certain boundary conditions we set before.

4.1 Basic Configuration

We decided to examine the axially symmetric problem of the electron positron system. Here we can reduce the dimension of the system further, ending up with a two dimensional lattice. We get few enough points, so that the memory usage is in manageable dimensions and the resolution is high enough.

From the three degrees of freedom only two remain. These are the functions $q_r(r, z)$ and $q_z(r, z)$ as defined in equation (3.1). The functions can vary between

zero and one. But the sum of the squares must not be bigger than one.

$$\begin{aligned} 0 \leq q_z(r,z) \leq 1 \\ 0 \leq q_r(r,z) \leq 1 \\ 0 \leq q_r(r,z)^2 + q_z(r,z)^2 \leq 1 \end{aligned} \tag{4.1}$$

We achieve this by the following parametrisation

$$\begin{aligned} q_r(r,z) &= \cos(x_{2n+1}) \tanh(x_{2n}) \\ q_z(r,z) &= \sin(x_{2n+1}) \tanh(x_{2n}) \end{aligned} \tag{4.2}$$

where we numbered all lattice points with $0 \leq n \leq N$ where N is the number of all lattice points that are varied. Now we can change the parameters x_n arbitrarily. We define the energy in the system as a function of all parameters

$$E = f(x_1, \ldots, x_{2N+1}) \tag{4.3}$$

When we already know the distribution of the $\mathbf{n}$-field from analytic calculations we can fix this degree of freedom. Then we leave the ratio q_r/q_z fixed and vary only $|\mathbf{q}| = \sqrt{q_r^2 + q_z^2}$ by setting

$$\begin{aligned} q_r(r,z) &= \cos(\theta) \tanh(x_n) \\ q_z(r,z) &= \sin(\theta) \tanh(x_n) \end{aligned} \tag{4.4}$$

where θ is the angle to the z-axis known from analytic calculations. In this way we have fewer parameters to vary. We can therefore make a step to larger lattices.

4.2 Calculation of the Energy

How do we get the energy out of our configuration on the lattice? First we have to know the energy density at every point. The energy density is a function of $q_r(r.z)$, $q_z(r,z)$ and the derivatives $\frac{\partial q_r(r,z)}{\partial r}$,$\frac{\partial q_z(r,z)}{\partial r}$,$\frac{\partial q_r(r,z)}{\partial z}$,$\frac{\partial q_z(r,z)}{\partial z}$. So we have to calculate the derivatives at every point on the lattice.

4.2.1 Derivatives on a Lattice

Let us first look at the one dimensional lattice. The easiest way to get a derivative is to take the difference between the values at neighboring points and divide by the lattice parameter. This includes two points.

$$\frac{df(x_n)}{dx} \approx \frac{f(x_n) - f(x_{n-1})}{a} \tag{4.5}$$

as a left derivative and

$$\frac{df(x_n)}{dx} \approx \frac{f(x_{n+1}) - f(x_n)}{a} \tag{4.6}$$

as the right derivative. We will use these derivatives on the boundaries, where we have only one neighboring point. A more accurate way is to take three points into account to calculate the derivative. We fit a parabola $g(x) = a+bx+cx^2$ into the three function values $f(x_{n-1})$, $f(x_n)$ and $f(x_{n+1})$. We then take the derivative of the fitted function $g'(x_n) = b + 2cx$ as an approximation of the derivative $f'(x_n)$. We get

$$\frac{df(x_n)}{dx} \approx \frac{f(x_{n+1}) - f(x_{n-1})}{2a}. \tag{4.7}$$

We can take this concept one step further and use five points (two points on each side of the point where we want to know the derivative). Here we fit a polynomial of order 4. We get

$$\frac{df(x_n)}{dx} \approx \frac{f(x_{n-2}) - 8f(x_{n-1}) + 8f(x_{n+1}) - f(x_{n+2})}{12a} \tag{4.8}$$

Wherever possible we use five points to calculate the derivative, only when we approach the boundary we have to reduce the number of points taken in to account.

4.2.2 Summation over the Lattice

On our two dimensional lattice we have to calculate partial derivatives. This is done by holding one coordinate fixed, while stepping one or two steps away in the other coordinate direction. Knowing the local energy density we have to carry out the integral over all lattice points. Each lattice point occupies the volume

$$V = 2\pi a^3 r \tag{4.9}$$

where we measure r in units of the lattice spacing. We have to make an exception at the origin. Here we assign the volume

$$V_O = \pi \left(\frac{a}{2}\right)^2 a = \frac{\pi a^3}{4} \tag{4.10}$$

With the energy density $\mathcal{H}(r, z)$ we can write the energy as

$$E = 2\pi a^3 \left(\frac{1}{8} \sum_{z=-Z}^{Z} \mathcal{H}(0, z) + \sum_{z=-Z}^{Z} \sum_{r=0}^{R} r\mathcal{H}(r, z) \right) \tag{4.11}$$

where the summation boundary Z is half the number of lattice points in z-direction and R the number of points in the r-direction.

We use the calculated energy as a function to be minimized by a computer program. There exist already a wide variety of ready made software packages to take this task off our hands. In our calculations we used the routines from Numerical Recipes [5], especially the routine for minimzing a function of several variables called POWELL. It implements Powell's method in multidimensions.

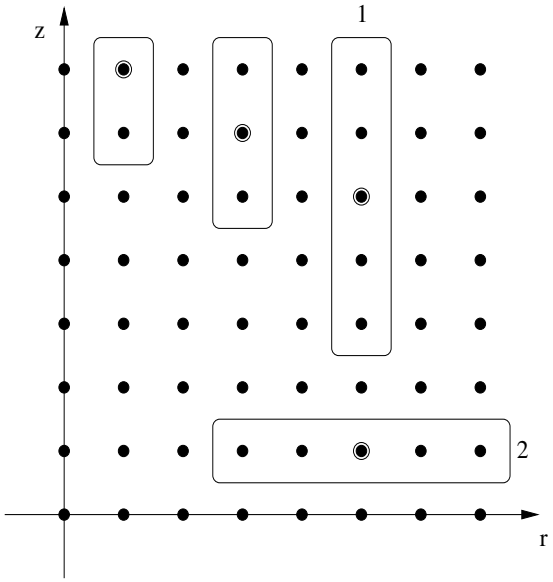

Figure 4.1: The derivatives are taken at the circled point. Depending on the position of the point the neighboring points are taken into account. 1) shows a partial derivative in z-direction, 2) in r-direction.

4.3 Boundary Conditions and Starting Configuration

Since we work with a finite volume we have to think about how the boundary influences the result. We actually know what we want to have at large distances: Maxwell's electrodynamics. We also know how the $\mathbf{n}$-field looks like at large distances from the soliton cores. But how big should we choose the volume and how do we fix the boundary?

We can make an estimate for the distance where the additional degree of freedom does not play a role anymore. Let us look at the one particle solution. Here we have

$$q_0 = \frac{r_0}{\sqrt{r_0^2 + r^2}} \tag{4.12}$$

Let us choose an upper bound for $q_0 < 10^{-2}$. At that value of q_0 the potential becomes negligible and also the $\mathbf{n}$-field has almost unit length ($|\mathbf{n}| > 0.99995$). Solving equation (4.12) for r we get $r > 10r_0$.

We want to start from a configuration that is already very close to the minimum, so the minimization process does not last very long. We already know the direction of the $\mathbf{n}$-field from equations (3.41) and (3.37). We only have to adjust the length of $\mathbf{q}$ ($\sqrt{1-q_0^2}$). Here we make a simple assumption. In the upper half plane ($z > 0$) we choose the distribution of q_0 to be the distribution of a single particle sitting at $z = d$. We do the same for the lower half plane. There will be discontinuities where the two solutions meet, but these will be evened out in the process of the minimization. In the

case where an analytic solution is known we can fix the direction of the $\mathbf{n}$-field.

4.4 Calculating the Energy Contribution Outside the Box

Outside the box we assume electrodynamics and therefore we can simply integrate over the energy density known from electrodynamics. The electric field of an electron positron pair sitting at $\pm d$ on the z-axis is

$$\mathbf{E} = \frac{e}{4\pi\epsilon_0}\left[\frac{1}{(r^2+(z+d)^2)^{3/2}}\begin{pmatrix} r \\ z+d \\ 0 \end{pmatrix} - \frac{1}{(r^2+(z-d)^2)^{3/2}}\begin{pmatrix} r \\ z-d \\ 0 \end{pmatrix}\right] \tag{4.13}$$

where we write $\mathbf{E}$ in cylindrical coordinates. We can already see that this is a complicated function and integrating $\mathbf{E}\cdot\mathbf{E}$ analytically will be difficult. So we try to do the integral

$$E = \frac{\epsilon_0}{2}\int d^3x\, \mathbf{E}\cdot\mathbf{E} \tag{4.14}$$

numerically. Unfortunately the integral converges very slowly, due to the choice of coordinates. To get a more accurate result we have to rewrite equation (4.14). Using $\mathbf{E} = \nabla\varphi$ with φ the electrostatic potential and $\nabla(\varphi\nabla\varphi) = \nabla\varphi\cdot\nabla\varphi + \varphi\triangle\varphi$ we get

$$E = \frac{\epsilon_0}{2}\int d^3x\, (\nabla(\varphi\nabla\varphi) - \varphi\triangle\varphi). \tag{4.15}$$

Since the space outside the box is charge free, the Laplace equation $\triangle\varphi = 0$ holds at every point. Therefore the second term vanishes and an integral over a divergence remains. Now we can use Gauss' law to rewrite this volume integral into a surface integral. We take the boundary surfaces to be the surface of the cylinder and the sphere at infinity. The fields vanish fast enough at infinity so we do not get a contribution from that surface. We have finally

$$E = \frac{\epsilon_0}{2}\oint_{cylinder} d^2\mathbf{f}\cdot\varphi\nabla\varphi = \frac{\epsilon_0}{2}\oint_{cylinder} d^2\mathbf{f}\cdot\mathbf{E}\varphi \tag{4.16}$$

Using

$$\varphi = \frac{e}{4\pi\epsilon_0}\left[\frac{1}{\sqrt{r^2+(z+d)^2}} - \frac{1}{\sqrt{r^2+(z-d)^2}}\right] \tag{4.17}$$

we can calculate the energy.

4.5 Problems due to Numerics

When we look at the expression for the energy density equations (3.16) and (3.23) we see the denominator has a root for $q_r(r,z)^2 + q_z(r,z)^2 = 1$. Approaching this value the denominator becomes very small and inaccuracies in the numerator are amplified. Taking a point at the boundary and varying the length of $\mathbf{q}$ we get the behavior shown in figure (4.2). The remedy to this problem is to select a cut-off value for $1 - q_r^2 - q_z^2$

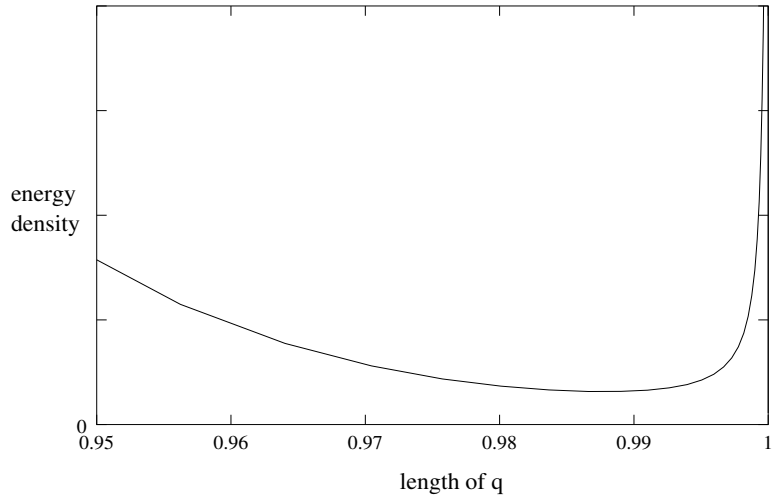

Figure 4.2: The behavior of the energy density for $|\mathbf{q}| \approx 1$. Shortly before reaching $|\mathbf{q}| = 1$ the energy density rises. That means this point can not be reached in the minimization process and therefore the minimum found may not be correct.

and use the electrodynamical approximation (equations (3.24) and (3.25)) from there on.

Chapter 5

Running Coupling

In quantum electrodynamics (QED) it is well known that the interaction characterized by the fine structure constant α gets stronger when one moves to distances smaller than the Compton wavelength $\lambda_c = 2.4226\,10^{-12}\,m$. In QED this effect is explained by vacuum polarization. The bare electron has charge infinity and induces a cloud of charges surrounding the electron. By this cloud the bare electron is shielded and at large distances one only sees the finite elementary charge $e_0 = 1.602\,10^{-19}\,C$. This effect has been confirmed by experiment up to a momentum transfer of $57.77\,GeV/c$. Then the fine structure constant takes a value of $\alpha(57.77\,GeV/c) = 128.6 \pm 1.6$ compared to the value at zero momentum transfer $\alpha(0) = 137.0359895 \pm 0.0000061$ (see [7]).

On the other hand we can look at the simple 1+1 dimensional sine-Gordon model. When two kinks collide the pendulums twist into each other, thereby increasing the potential energy in the system. This can be interpreted a strengthening of the coupling between the two kinks. We will also call this running coupling.

A similar effect can be observed in the MTF. Here we also have a potential energy that only surfaces at short distances (order of $r_0 = 2.21\,fm$ for the parameter $m = 3$). Therefore we expect also a "running coupling" effect in the MTF.

5.1 The Sine-Gordon Model

5.1.1 Short Introduction to the Model[1]

The sine-Gordon model is essentially a chain of spring-coupled pendula under the influence of gravity, where we take the limit to a continuous distribution of the pendulums. Then the behavior of the chain is governed by the differential equation

$$\frac{\partial^2\theta}{\partial t^2} - c_0\frac{\partial^2\theta}{\partial x^2} + \omega_0^2\sin\theta = 0 \tag{5.1}$$

This is the Klein-Gordon equation where the potential term is replaced by $\sin\theta$. Hence the name sine-Gordon model. The equation is non-linear and therefore allows solu-

tions unknown for the linear sine-Gordon equation. We can make the substitutions

$$T = \omega_0 t \qquad X = \frac{\omega_0}{c_0} x \tag{5.2}$$

Then the sine-Gordon equation becomes

$$\frac{\partial^2 \theta}{\partial T^2} - \frac{\partial^2 \theta}{\partial X^2} + \sin\theta = 0 \tag{5.3}$$

We can also introduce a normalized velocity u and a moving coordinate frame $s = X - uT$. Then the simplest solution is

$$\theta = 4 \arctan\left(e^{\pm \frac{s - s_0}{\sqrt{1-u^2}}}\right) \tag{5.4}$$

The opposite signs in the exponent indicate the different screw sense and can be identified with the kink and the anti-kink solution. We will also call the factor

$$\frac{1}{\sqrt{1+u^2}} = \gamma \tag{5.5}$$

since it is similar to the γ known from special relativity. The moving kinks also show Lorentz contraction and the energy stored in the kink increases. The energy present in the system is given by

$$E = \omega_0 c_0 \int_{-\infty}^{\infty} \frac{1}{2} \left(\left(\frac{\partial \theta}{\partial T}\right)^2 + \left(\frac{\partial \theta}{\partial X}\right)^2 \right) + (1 - \cos\theta)\, dX \tag{5.6}$$

in the dimensionless units X and T. We can plug the kink-solution equation (5.4) in (5.6) and get the energy for a single soliton

$$E = 8\gamma\omega_0 c_0 = \gamma m_0 c_0^2 \tag{5.7}$$

with

$$m_0 = 8\frac{\omega_0}{c_0} \tag{5.8}$$

There also exist solutions for the kink-kink collision and the kink-antikink collision. The one for the kink-kink collision is in dimensionless variables

$$\theta(X,T) = 4 \arctan\left(u \sinh(\gamma X) \mathrm{sech}(\gamma u T)\right) \tag{5.9}$$

and the one for kink-antikink collision

$$\theta(X,T) = 4 \arctan\left(\frac{1}{u} \mathrm{sech}(\gamma X) \sinh(\gamma u T)\right) \tag{5.10}$$

The nature of the localized solitons can be seen best when we look at the spatial derivative of the function $\theta(X,T)$. Here we get

$$\frac{\partial \theta}{\partial X} = \frac{4u}{\sqrt{1-u^2}} \frac{\cosh(\frac{X}{\sqrt{1-u^2}})\mathrm{sech}(\frac{uT}{\sqrt{1-u^2}})}{1 + u^2 \mathrm{sech}^2(\frac{uT}{\sqrt{1-u^2}}) \sinh^2(\frac{X}{\sqrt{1-u^2}})} \tag{5.11}$$

We can plot this for a fixed u at different times.

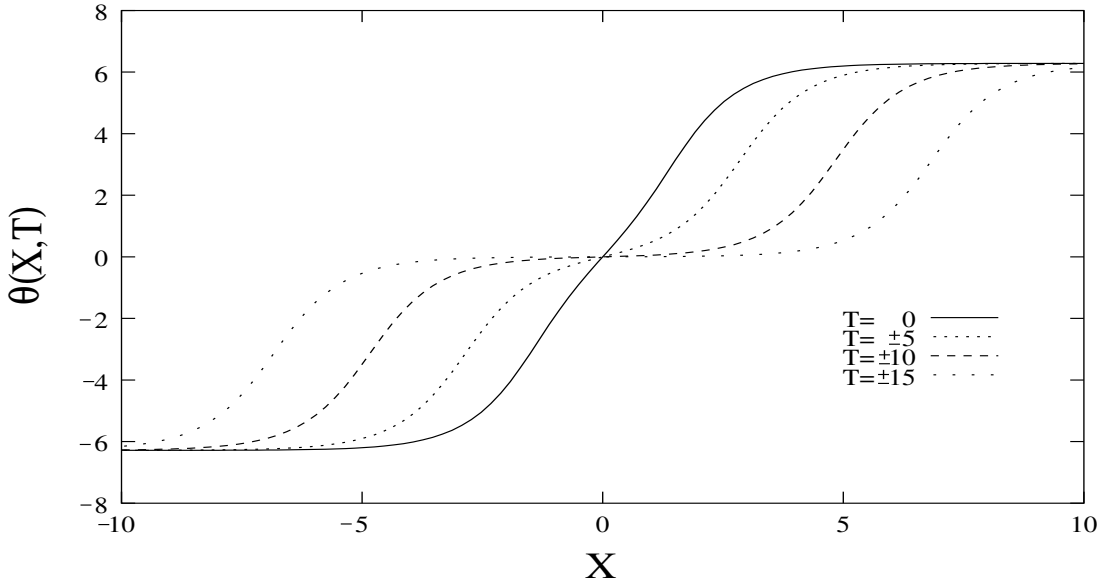

Figure 5.1: The profile function $\theta(X,T)$ shown at different times T for $u = 0.4$. At large negative times each kink is independent and looks almost like a single kink. In the vicinity of $T = 0$ the kinks start interacting and repel each other. At large positive times they are independent again.

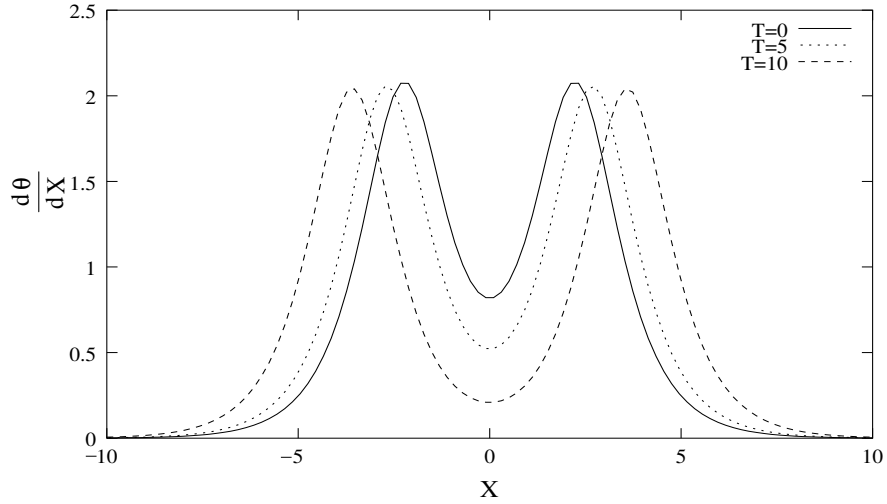

Figure 5.2: The derivative of the profile function $\frac{\partial\theta}{\partial X}$ at different times for $u = 0.2$. Here we see the localized nature of the kinks more clearly. We can also see that for close distances the derivative does not reach zero between the two kinks.

5.1.2 Running Coupling in the Sine-Gordon Model

If we want to talk about running coupling we have to define a distance between the two kinks first. We measure the distance between the centers of the kinks, defining

the center of the kink as the point with $\theta = \pm\pi$. At $T = 0$ the kinks are closest, all the kinetic energy is stored in potential energy. We want to plot the energy in the system as a function of the distance of the kinks at this point, where we can set $E_{pot} = E_{kin} = 2m_o c^2(\gamma - 1)$. We take equation (5.9) at $T = 0$

$$\theta(X, 0) = 4 \arctan\left(u \sinh(\gamma X)\right) \tag{5.12}$$

and using

$$u = \frac{\sqrt{\gamma^2 - 1}}{\gamma} \tag{5.13}$$

we can solve equation (5.12) we get as condition for the minimum distance

$$\pi = 4 \arctan\left(\frac{\sqrt{\gamma^2 - 1}}{\gamma} \sinh(\gamma X_{min})\right). \tag{5.14}$$

This involves γ in a very complicated way, so we can not explicitely solve for it. Trying to solve the equation numerically we get Figure (5.3). But we can try to solve this in a certain limit. Since X_{min} and γ are interdependent let us first separate them and solve for X_{min}.

$$X_{min} = \frac{1}{\gamma} \text{arsinh}(\frac{\gamma}{\sqrt{\gamma^2 - 1}}) \tag{5.15}$$

For large γ we can expand (5.15) in terms of $1/\gamma$ and get

$$X_{min} = \frac{\sinh(1)}{\gamma} \qquad \text{or} \qquad \gamma = \frac{\sinh(1)}{X_{min}} \tag{5.16}$$

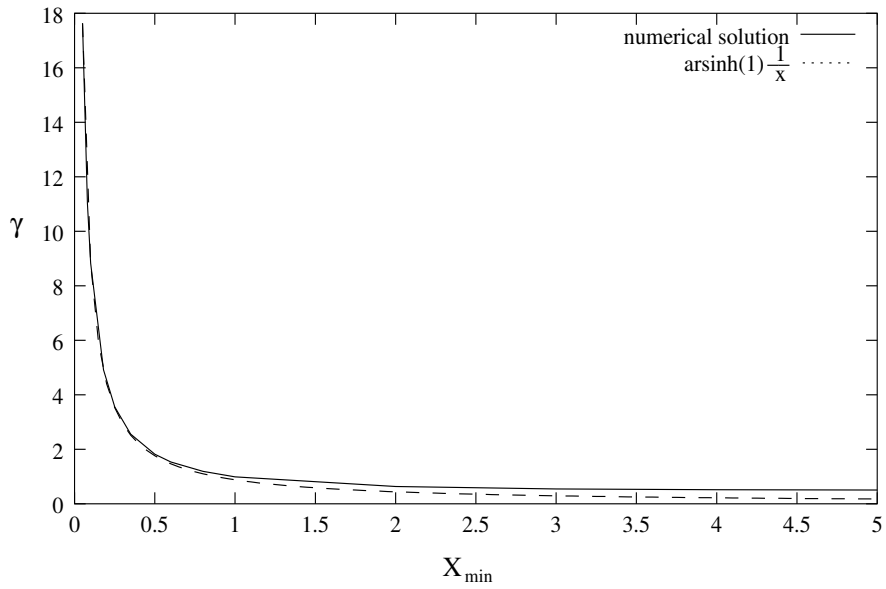

Figure 5.3: The energy in the system as a function of the closest distance of the two kinks. For small distances the curve approaches equation (5.16). For large distances it approaches 1.

Chapter 6

Results

6.1 Preparations

To use a computer program for our minimization we had to put the problem on a lattice. We discussed the lattice size in Chapter 4. So, depending on the distance between the centers of the particles, we chose a different lattice size. To get reasonable smooth derivatives we chose the parameter $r_0 = 3a$ where a is the lattice spacing.

We will calculate all energies in units of the inverse lattice spacing. They translate to SI-Units in the following way.

$$E_{SI} = \frac{\alpha_f \hbar c}{a} E_a \tag{6.1}$$

For the parameter $m = 3$ we already know the length of r_0 and therefore the conversion factor.

We want to compare the two particle energy with the energy of two separated particles. Therefore we have to calculate the energy of a single particle. We will do this numerically, despite the known analytic solution. If we later take the difference to the two particle energies some errors will cancel. We chose a lattice size of 61x30 points (that leaves $10r_0$ in every direction from the center) in accord with Chapter 4. The results are shown in Table 6.1. When we compare this energy now with the rest

	Energy in the box	Energy outside	Total energy	Analytic result
1	$2.470703 \cdot 10^{-1}$	$0.148122 \cdot 10^{-1}$	$2.618825 \cdot 10^{-1}$	$2.617994 \cdot 10^{-1}$
2	$8.857895 \cdot 10^{-1}$	$0.148122 \cdot 10^{-1}$	$9.006017 \cdot 10^{-1}$	—

Table 6.1: The rest energy of one particle (E_1) in units of $\frac{\alpha_f \hbar c}{a}$. The energy inside the box was calculated by a C computer program, minimizing the energy in the box while holding the $\mathbf{n}$-field constant. The result for the outside was also calculated numerically, but here with MATHEMATICA using equation (4.16). For line 1 the parameters are $m = 3$, $r_0 = 3a$, for line 2 $m = 1$, $r_0 = 1.5a$.

mass of the electron we can calculate the lattice spacing. Solving equation (6.1) for the lattice constant we get

$$a = E_a \frac{\alpha_f \hbar}{m_0 c} \tag{6.2}$$

where m_0 is the rest mass of the electron. For the two cases in Table 6.1 we get

	a
$m = 3,\ r_0 = 3a$	$7.38163 \cdot 10^{-16}\, m$
$m = 1,\ r_0 = 1.5a$	$2.53851 \cdot 10^{-15}\, m$

6.2 Energies for the interacting particles

We now add the energies coming from the computer program with the energies outside the box for the two particles states. We always chose the lattice in such a way that the distance from a soliton core to the boundary was always 30 lattice units (= $10r_0$). Since we want to investigate the non-linear behavior of the particles we have to choose our distance range accordingly. We expect a departure from the usual Coulomb law for distances smaller than 30 lattice units. Above this distance the energy in the system should approach double the rest mass minus the interaction energy known from electrodynamics. Therefore we chose a distance range from 105 units down to 15 units. The results are shown in Table 6.2. . To get a better view at the running coupling we will calculate the effective charge from the system energy. Therefore we introduce a function $Q(r)$ to model the behavior of the energy. If we write the energy in units of $\frac{\alpha_f \hbar c}{a}$ we get

$$E = 2E_1 - \frac{Q^2(r)}{r}. \tag{6.3}$$

The effective charge $Q(r)$becomes

$$Q(r) = \sqrt{(2E_1 - E)r} \tag{6.4}$$

Using the numerical values in this equation we get Figure 6.2.

The energy difference between the two toplogically different states is shown in Figure 6.4.

Lattice	Distance	Energy inside	Energy outside	Total Energy
73x30	12	0.4323675	0.0009726	0.43334014
75x30	14	0.4466906	0.0012843	0.44797490
79x30	18	0.4639817	0.0019996	0.46598133
85x30	24	0.4781735	0.0032483	0.48142183
91x30	30	0.4856624	0.0046271	0.49028945
97x30	36	0.4899537	0.0060576	0.49601126
103x30	42	0.4925416	0.0074792	0.50002079
109x30	48	0.4941228	0.0088494	0.50297223
115x30	54	0.4951294	0.0101418	0.50527120
121x30	60	0.4957696	0.0113425	0.50711210
127x30	66	0.4961729	0.0124465	0.50861940
133x30	72	0.4964215	0.0134549	0.50987640
139x30	78	0.4965687	0.0143721	0.51094080
151x30	90	0.4966859	0.0159599	0.51264580
165x30	105	0.4966770	0.0176172	0.51429370

Table 6.2: The results for the numerical calculation of the interaction energy of a positron electron interaction for the case $m = 3$, $r_0 = 3a$. The particles are fixed at the given distance. The graphical representation is given in Figure 6.1.

Lattice	Distance	Energy inside	Energy outside	Total Energy	Difference to other
73x30	12	0.4327904	0.0009726	0.43376304	$4.2290 \cdot 10^{-4}$
79x30	18	0.4640872	0.0019996	0.43376304	$1.0550 \cdot 10^{-4}$
85x30	24	0.4640872	0.0032483	0.48145803	$3.6200 \cdot 10^{-5}$
91x30	30	0.4856781	0.0046271	0.48145803	$1.5700 \cdot 10^{-5}$
97x30	36	0.4899608	0.0060576	0.49601836	$7.1000 \cdot 10^{-6}$
103x30	42	0.4925416	0.0074792	0.49601836	$> 10^{-7}$
109x30	48	0.4925416	0.0088494	0.50297223	$> 10^{-7}$
115x30	54	0.4951294	0.0101418	0.50527120	$> 10^{-7}$
121x30	60	0.4951294	0.0113425	0.50711210	$> 10^{-7}$
127x30	66	0.4961729	0.0124465	0.50711210	$> 10^{-7}$
133x30	72	0.4961729	0.0134549	0.50987640	$> 10^{-7}$
139x30	78	0.4965687	0.0143721	0.51094080	$> 10^{-7}$
151x30	90	0.4965687	0.0159599	0.51264580	$> 10^{-7}$
165x30	105	0.4966777	0.0176172	0.51429490	$> 10^{-7}$

Table 6.3: Here are the numerical results for the topological state where the soliton cores lie at different poles of the S^3. The energy lies a little higher than the energy for the state where both centers lie on the same pole. Also the energy difference to the other state is given. The graphical representation is given in Figure 6.3.

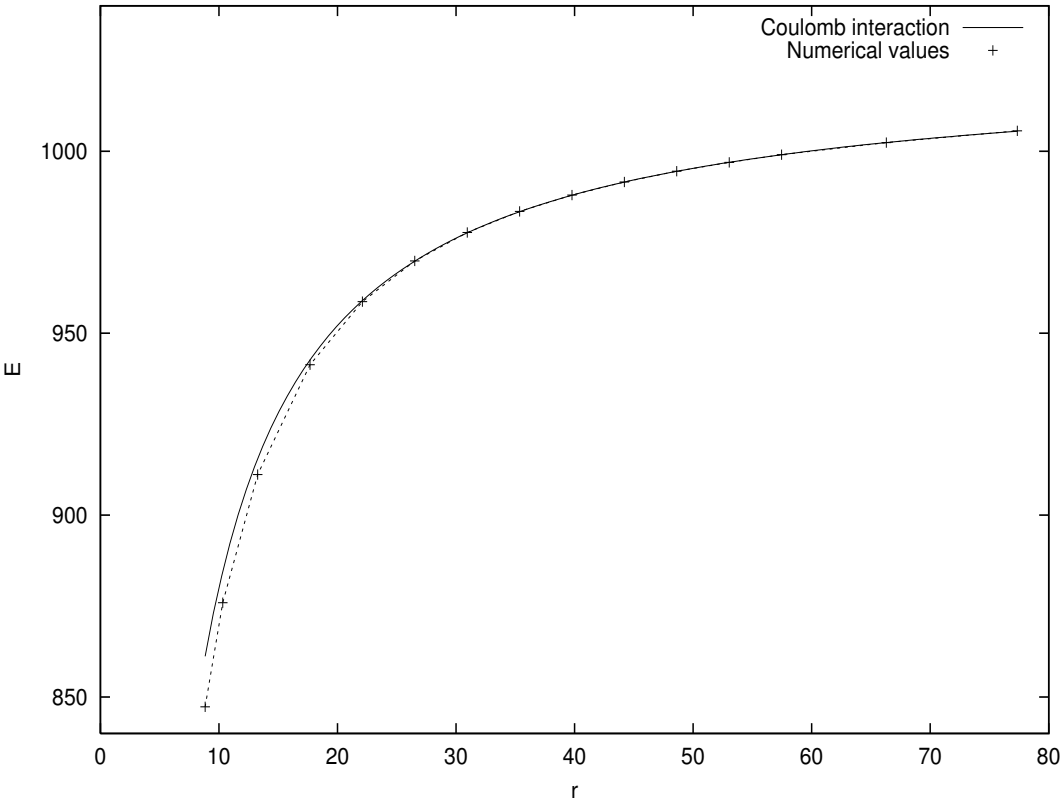

Figure 6.1: The behavior of the total energy in the system E_{tot} compared to two times the rest mass plus the potential of the Coulomb interaction. The energy values are given keV, the radius is given in fm.
For large distances ($r > 10r_0$) one can see how the energy approaches the value known from Coulomb interaction. . When the distance becomes smaller than $10r_0$ it departs from the Coulomb curve and takes a slightly lower value. If one does not know of the extended nature of the particle this drop in the potential energy can be interpreted as the strengthening of the coupling constant α_f for small distances.

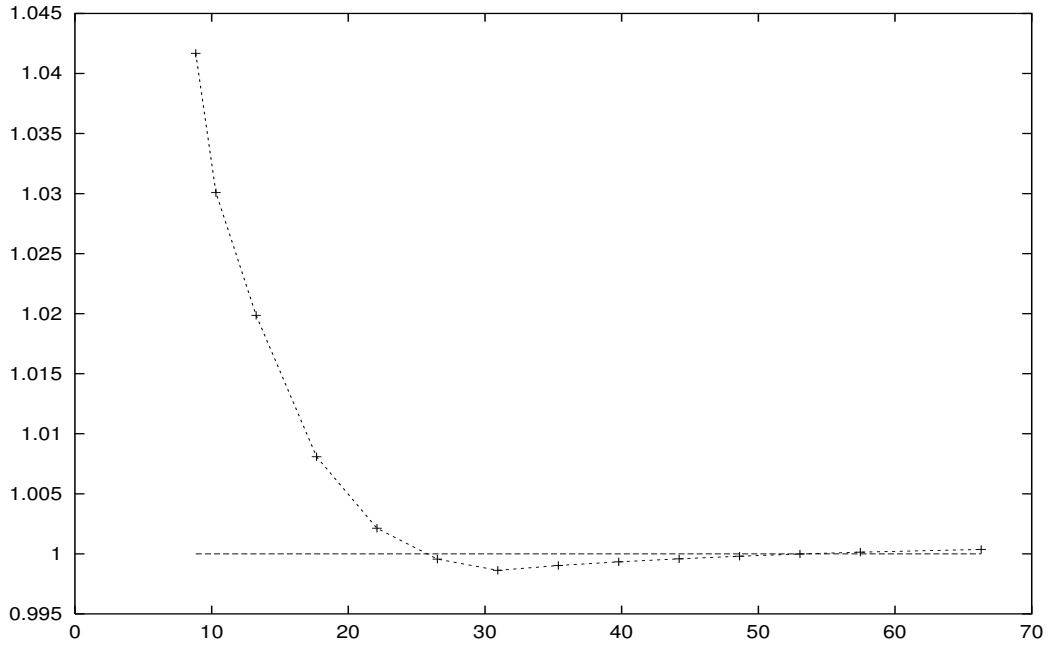

Figure 6.2: The effective charge in units of the elementary charge as a function of the distance (in fm). We see a clear running coupling effect for short distances. For longer distances the calculation is not accurate enough, so the curve dips slightly below 1. We suspect the influence of the finite lattice size. The effect is much stronger than the predicted value from QED and also the incline is stronger.

Lattice	Distance	Energy inside	Energy outside	Total Energy
73x30	12	1.7170720	0.0009726	1.7180446
79x30	18	1.7439370	0.0019996	1.7459366
85x30	24	1.7565410	0.0032483	1.7597893
91x30	30	1.7634460	0.0046271	1.7775092
97x30	36	1.7675250	0.0060576	1.7735826
103x30	42	1.7700300	0.0074792	1.7775092
109x30	48	1.7716010	0.0088494	1.7804504
115x30	54	1.7725940	0.0101418	1.7860615
121x30	60	1.7732220	0.0113425	1.7845645
127x30	66	1.7736150	0.0124465	1.7860615
133x30	72	1.7738550	0.0134549	1.7873099
139x30	78	1.7739950	0.0143721	1.7883671
151x30	90	1.7741020	0.0159599	1.7900619
165x30	105	1.7740860	0.0176172	1.7917032

Table 6.4: The energies for the case $m = 1$, $r_0 = 1.5a$, again in units of $\frac{\alpha_f \hbar c}{a}$. The graphical representation is given in Figure 6.4.

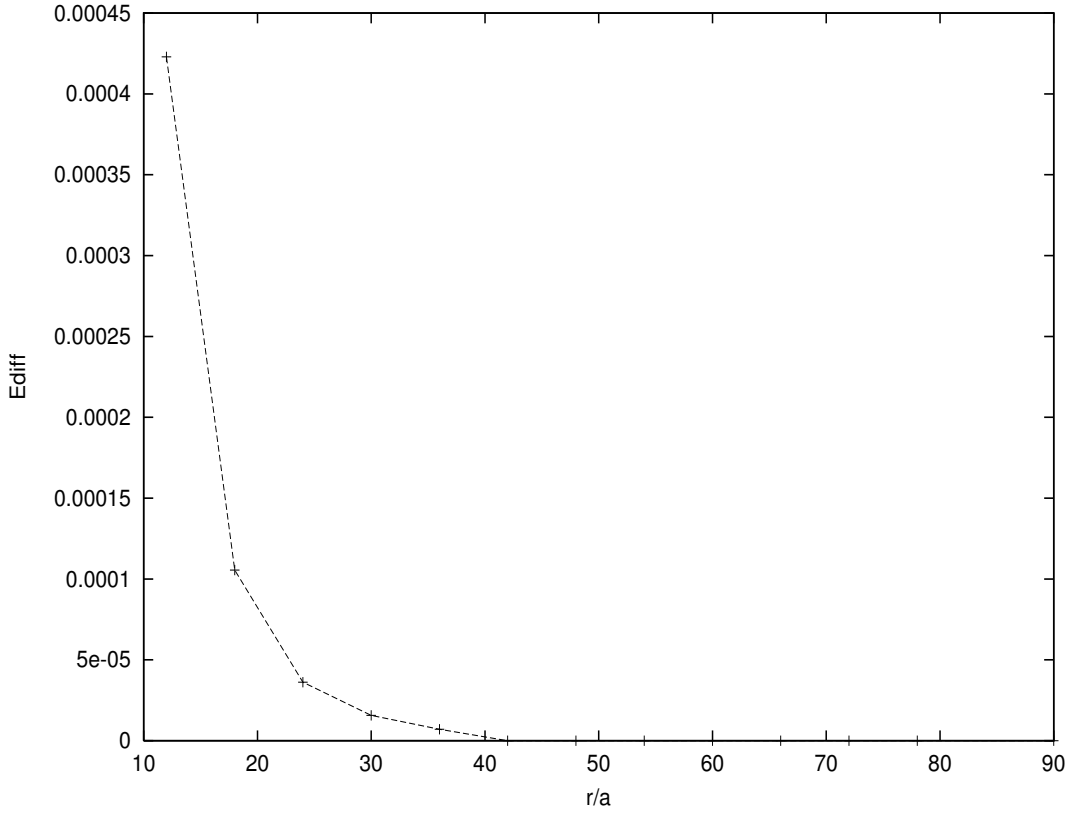

Figure 6.3: The energy difference E_{diff} between the two topological states in units of $\frac{\alpha_f \hbar c}{a}$. The difference seems to obey a power law. The error mentioned before would be larger than the plotted values, but since we made the calculations on the same lattice the errors cancel.

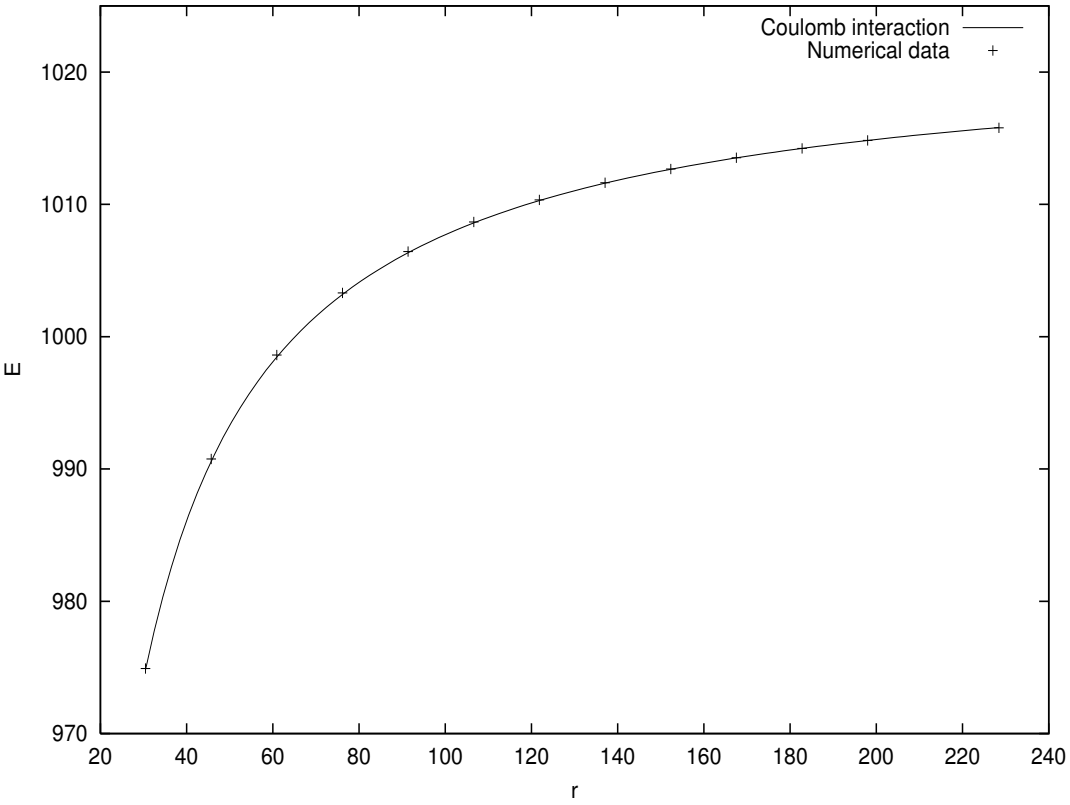

Figure 6.4: The numerical values for the total system energy for the case $m = 1$, $r_0 = 1.5a$. The distance is given in units of fm, the energy in units of keV. Since we are at larger distances compared to the case $m = 3$, $r_0 = 3a$ we do not see a running coupling effect yet. The accuracy is not high enough to show a running coupling effect at these distances. In our calculations all energies are of the order of the rest mass of the electron. The energy difference here is much to small to be discernible. Also the energy density for this case is more localized at one point (see Figure A.3). Therefore we expect the running coupling effect to start at smaller distances than for $m = 3$, $r_0 = 3a$.

Chapter 7

Conclusion and outlook

Remodeled Electrodynamics

Maxwell's electrodynamics does not know of quantized charges. Any charge distribution is allowed. We know that in nature a charge distribution is only an approximation and that all charges are built out of seemingly pointlike elementary particles. If we consider a SU(2) gauge theory with a potential that allows the formation of solitons, we recognize some of the properties of electrons in these solitons. The theory should not collide with existing knowledge, so in the limit for large distances Maxwell's theory should come out of the model.

We showed that this is the case. The topological constraints led to the inhomogeneous Maxwell equations where only quantized point charges are allowed. The variation of the remaining degrees of freedom in the limit of large distances $r \gg r_0$, where r_0 is a length scale inherent to the model, give the homogenous Maxwell equations.

We can choose a special gauge, so that the connection of the underlying SU(2) field coincides with the dual potential from electrodynamics. We apply a special rotation to the field, such that it is aligned in 3-direction. The 3-component of the connection becomes the dual potential. If we apply rotations about the direction in which the field is pointing we do not change anything. This is the U(1) gauge invariance known from electrodynamics. This knowledge allows the calculation of the soliton field out from a known potential.

Nonlinear Effects

We looked at a special effect of the nonlinearity of the sine-Gordon model. When two kinks come close, their potential energy departs from the long range behavior as a cause of the extended nature of the kinks. We showed that the same effect can be observed in the MTF. Due to the similarity to the effect in QED we suggest the name "running coupling" for it. Compared to the effect from QED our "running coupling" effect is larger and also seems to have a different functional dependence on the radius.

Inspired from the correspondence between the sine-Gordon model and the quantum-fieldtheoretical Thirring model we suggest there may exist the same correspondence

between QED and a four dimensional model with solitons. Our model is a first step in this direction. If a correspondence exists this mechanism could be the way that running coupling emerges from a soliton model.

Different States

We were able to show that there exists an energy difference between two possible topological states of a soliton-antisoliton system. In nature we observe a similar energy difference between two possible spin states of an two particle system. We suspect there is a connection between these two effects. There are still further investigations necessary to explain this possible connection.

Summary

We get some interesting features out of this simple attempt to describe electrons as solitons:

- Out of the MTF we get Maxwell's electrodynamics with quantized charges. At long ranges the theories are equivalent.
- Since the particles are not pointlike, but extendend objects, additional effects can be observed.
- It is possible to get an effect similar to running coupling out of a classical field theory.
- There seems to be a discrete energy difference between two possible states, maybe a model for spin.

Appendix A

Field configurations and Pictures

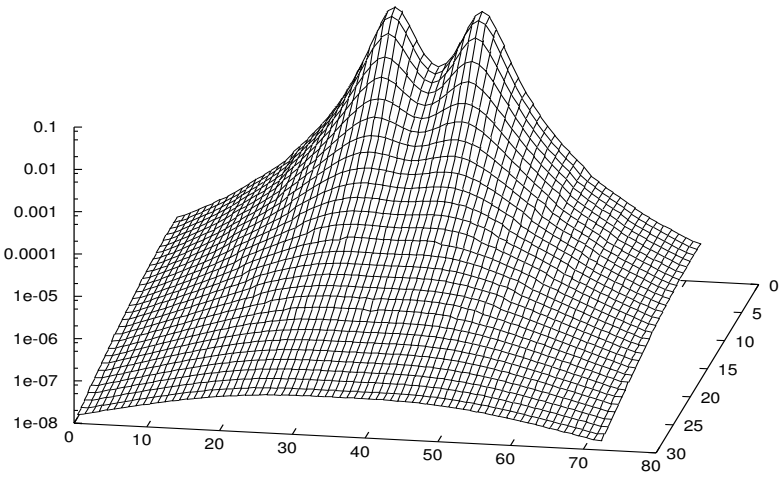

Figure A.1: The energy density for the case $m = 3\,r_0 = 3a$ on a logarithmic scale as a function of the radius and the-z coordinate. The parameters for this plot are $m = 3$, $r_0 = 3a$ and the distance between the particles $d = 12a$. When we compare this with the behavior of point particles we see, that for an extended object it is possible that a part of the particle is "cut off" and the field energy from this part is missing. For a point particle this is not possible, since the mass is concentrated at a single point. In an extended system the particles overlap and for close distances the function departs from a solution where we simply superimpose the two one particle solutions. The energy density in the overlap part is lower than the energy density in the superimposed solution. This is the origin of the reduced system energy at close distances.

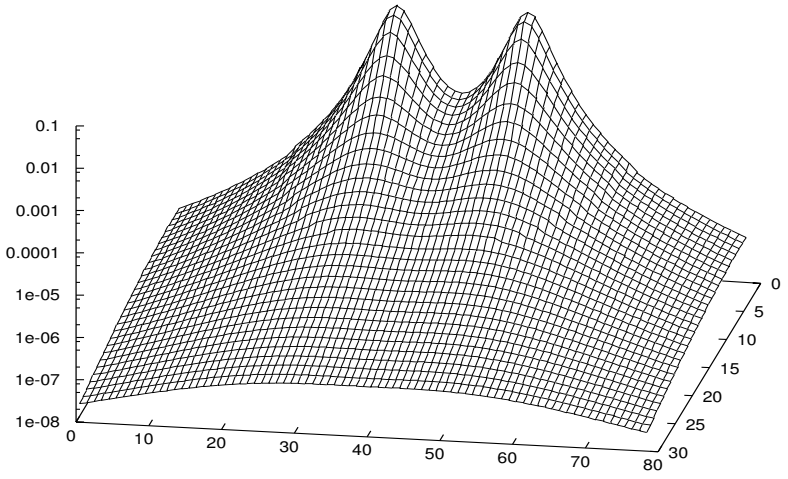

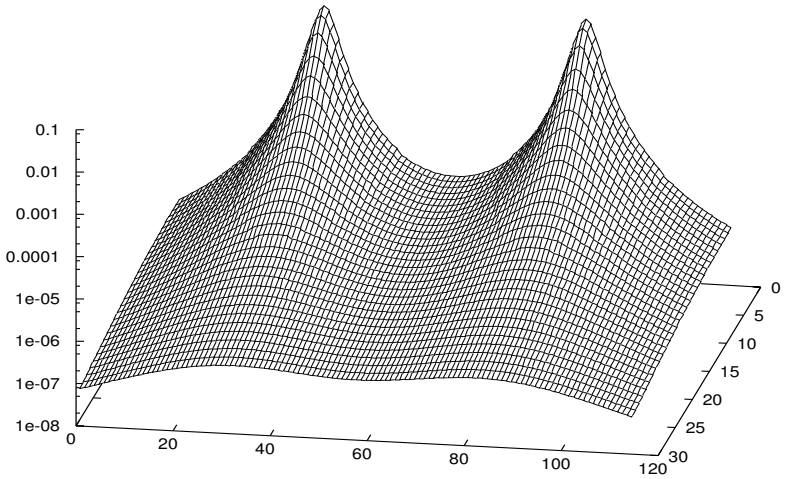

Figure A.2: The energy density as in Figure A.1, but for a larger distances between the particles ($d = 18a$, $d = 54a$). When the distance grows, the saddle point becomes lower and each particle more defined.

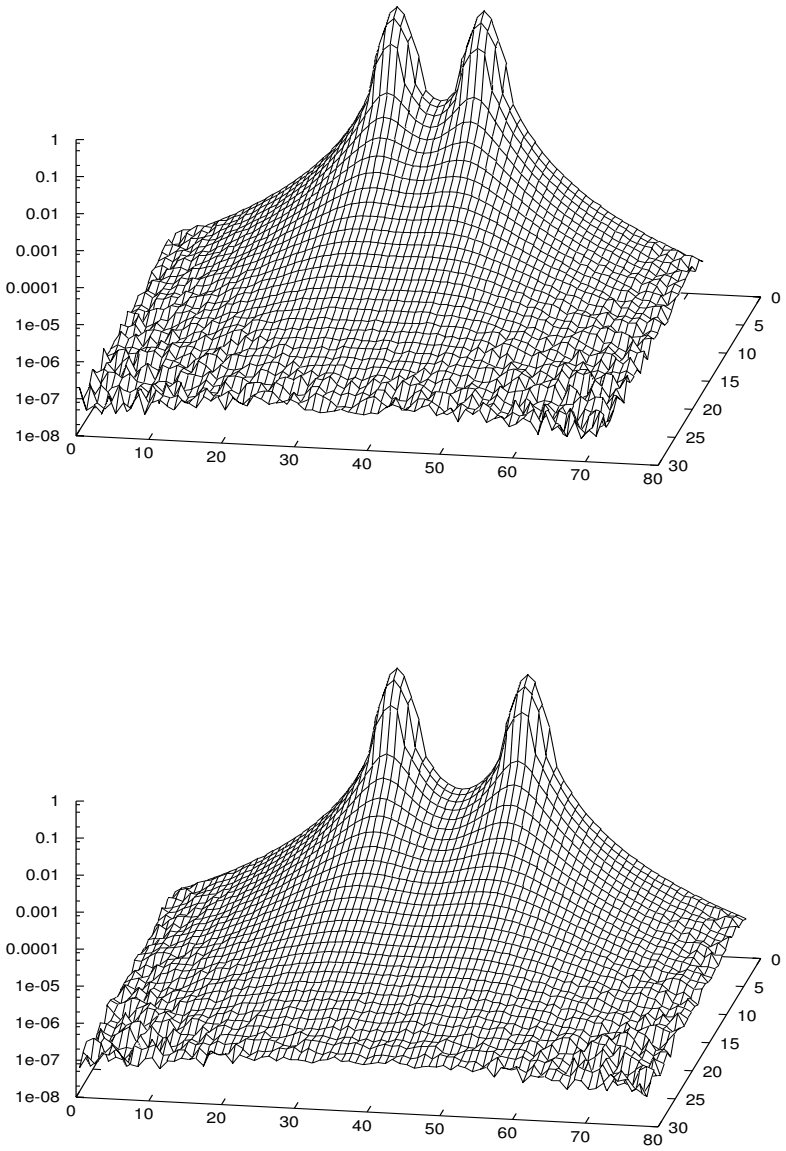

Figure A.3: The energy density plots for $m = 1$, $r_0 = 1.5a$ and a distance of 12 and 18 lattice constants. The particles are localized stronger than for $m = 3$. Most of the energy is concentrated in a small volume around the core. Outside this volume the energy density falls fast (note that the plot is logarithmic). One can also see the inaccuracies starting at small numbers, forming a "noisy" underground.

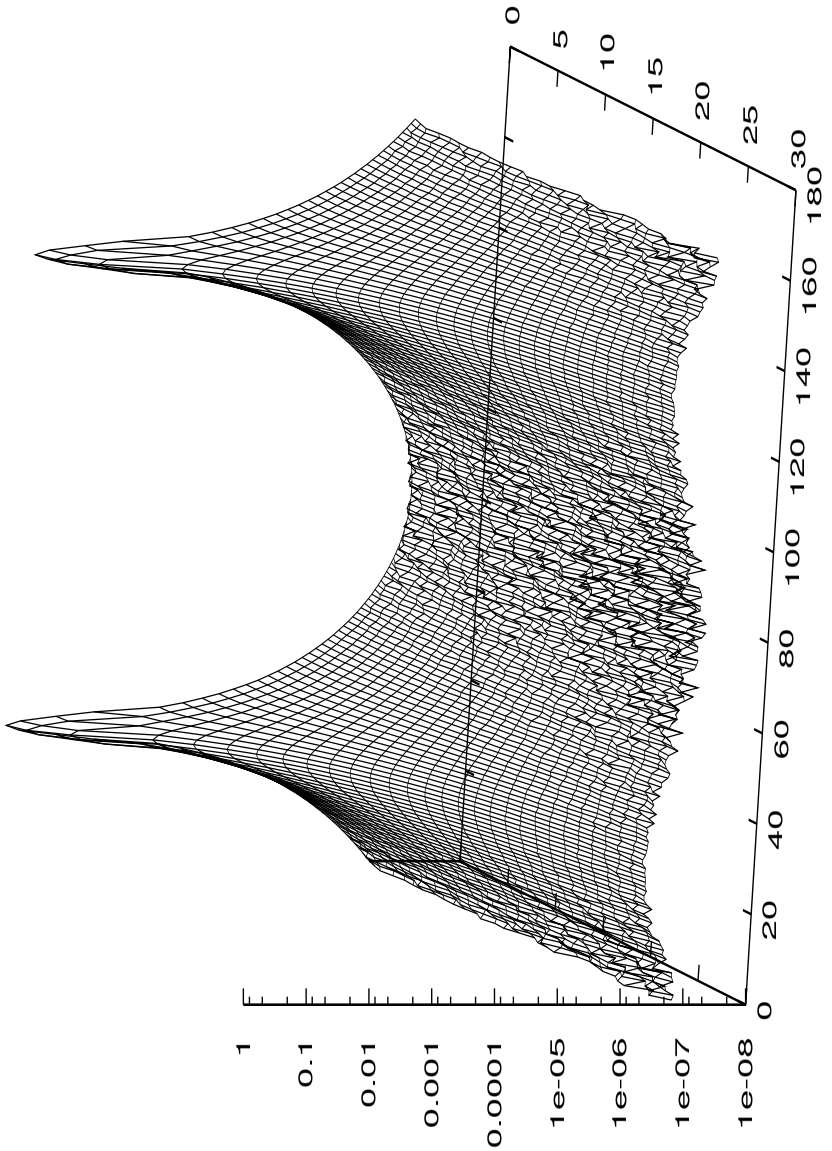

Figure A.4: The energy density for $m = 1$, $r_0 = 1.5a$ and a distance of 105 lattice units.

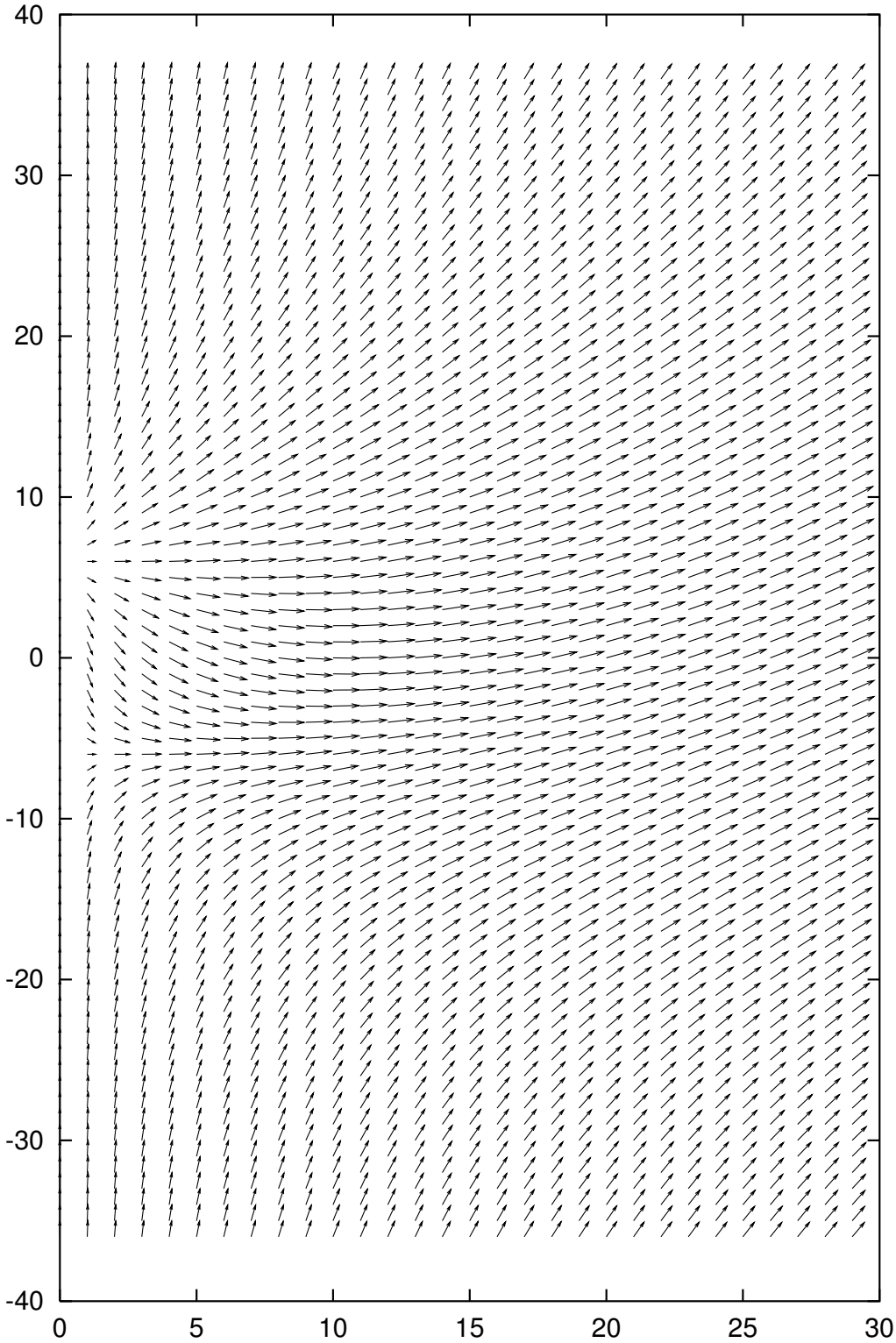

Figure A.5: Field configuration for $m = 3$, $r_0 = 3$ and d=12 lattice units. The lattice size is 73×30.

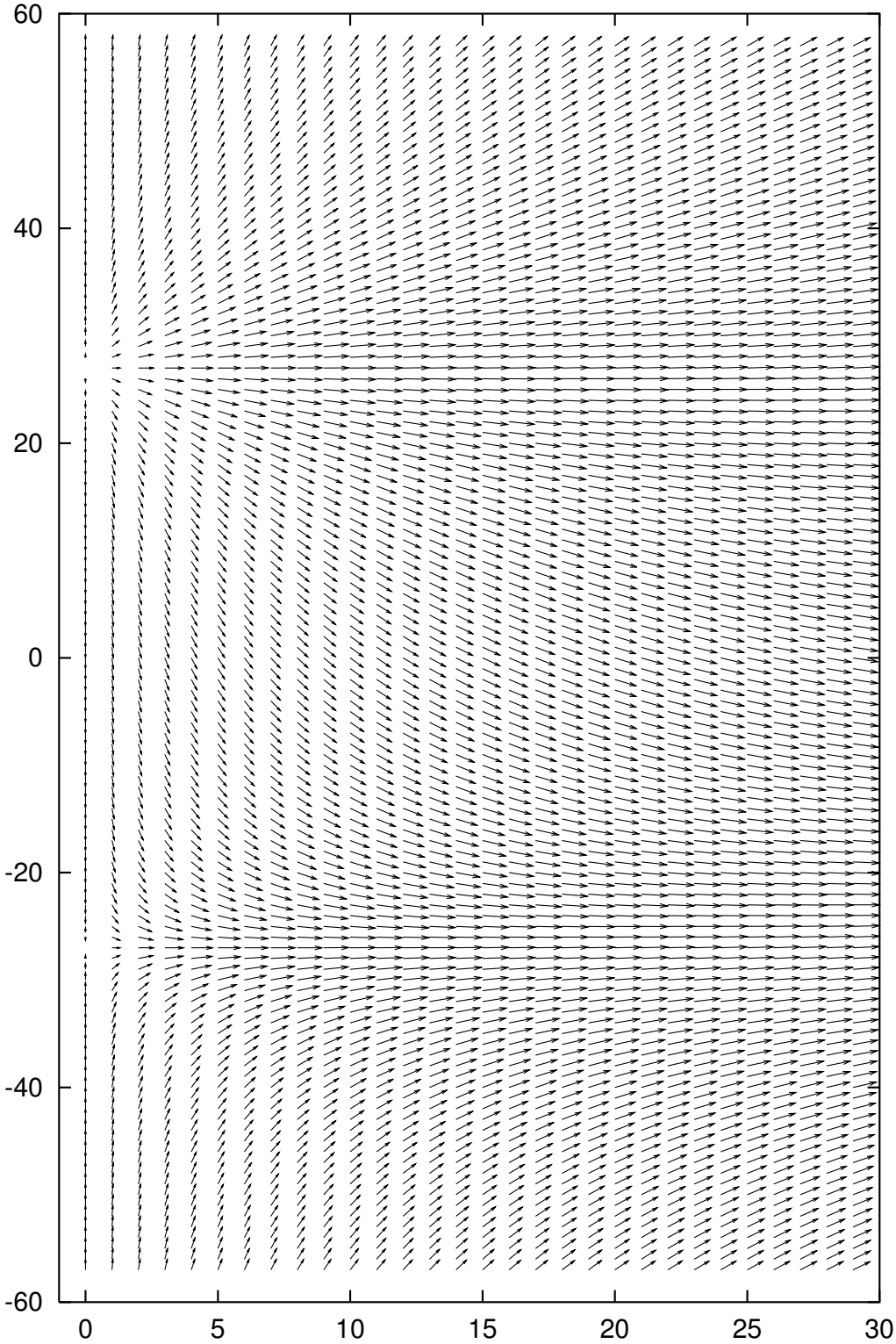

Figure A.6: Field configuration for $m = 3$, $r_0 = 3$ and d=54 lattice units. The lattice size is 115×30.

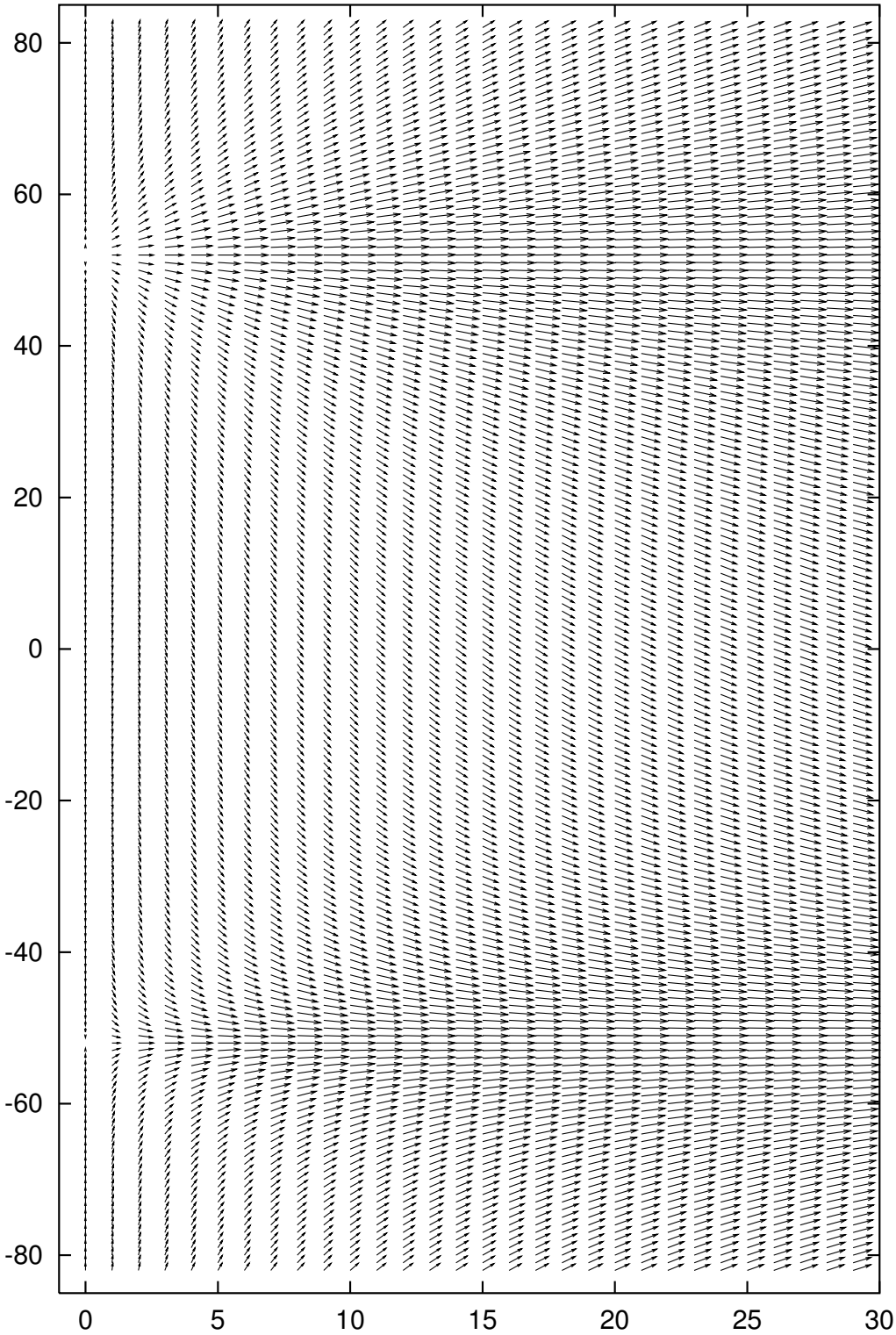

Figure A.7: Field configuration for $m = 3$, $r_0 = 3$ and d=105 lattice units. The lattice size is 165×30.

Bibliography

[1] M. Remoissenet, Waves Called Solitons, Concepts and Experiments, Springer, Berlin 1994.

[2] M. Faber, "A model for topological fermions," Few Body Syst. **30** (2001) 149 [hep-th/9910221].

[3] M. Baker, J. S. Ball, and F. Zachariasen, "Classical electrodynamics with dual potentials", [hep-th/9403169].

[4] R. A. Bertlmann, "Anomalies in quantum field theory," *Oxford, UK: Clarendon (1996) 566 p. (International series of monographs on physics: 91).*

[5] W.H. Press, S.A. Teukolsky, W.T. Vetterling, B.P. Flannery, Numerical Recipes in C, Cambridge University Press, Cambridge 1992.

[6] H. Chan, S. T. Tsou, Some Elementary Gauge Theory Concepts, World Scientific Lecture Notes in Physics, Singapore 1993.

[7] I. Levine *et al.* [TOPAZ Collaboration], "Measurement of the electromagnetic coupling at large momentum transfer," Phys. Rev. Lett. **78** (1997) 424.